Original Article

Landscape and climatic features drive genetic differentiation processes in a South American coastal plant

GUSTAVO A. SILVA-ARIAS[1,2], LINA CABALLERO-VILLALOBOS[1], GIOVANNA C. GIUDICELLI[1], LORETA B. FREITAS[1*]

[1]*Laboratory of Molecular Evolution, Department of Genetics, Universidade Federal do Rio Grande do Sul, Porto Alegre, RS, Brazil.*

[2] *Section of Population Genetics, Center of Life and Food Sciences Weihenstephan, Technische Universität München, Liesel-Beckmann-Straße 2 85354 Freising, Germany.*

[*]For correspondence. E-mail: loreta.freitas@ufrgs.br

Genetic differentiation in South America´s coastline

ABSTRACT

Background and aims Historical and ecological processes shaped the patterns of genetic diversity in plant species; among these, colonization to new environments such as coastal regions generate multiple signals of interest to understand the influence of landscape features on the population differentiation.

Methods We analysed the genetic diversity and population structure of *Calibrachoa heterophylla* to infer the influence of abiotic landscape features on this coastal species' gene flow in the South Atlantic Coastal Plain (SACP). We used ten microsatellite loci to genotype 253 individuals from 15 populations, covering the species' entire geographical range. We applied population genetics analyses to determine population diversity and structure along the SACP, migration model inference and correlative analyses to disentangle the most likely drivers of gene flow in the SACP.

Key Results The *C. heterophylla* populations located more distantly from the seashore showed higher genetic diversity than those closer to the sea. The genetic differentiation had a consistent signal of isolation-by-distance. Landscape features, such as water bodies and wind corridors, and raw geographical distances equally explained the genetic differentiation, whereas the precipitation seasonality showed a strong signal for isolation-by-environment in marginal populations. The estimated gene flow suggested that marginal populations had restricted immigration rates, which could enhance the genetic differentiation.

Conclusions The influence of topographical features in population differentiation in *C. heterophylla* is related with the history of the coastal plain deposition. Gene flow is mainly restricted to nearby populations and facilitated by wind fields but with no apparent influence of large water bodies. Furthermore, differential rainfall regimes in marginal populations can promote local genetic differentiation.

Key words: *Calibrachoa heterophylla; c*oastal species; colonization; gene flow; landscape genetics; Solanaceae; South Atlantic Coastal Plain.

INTRODUCTION

Coastal areas in South America constitute distinct landscapes with unique biotic composition. Many different geomorphological, climate, oceanographic features, and colonization events from the surrounding biomes shaped these areas (Hulton *et al.*, 2002; Scarano, 2002; Behling, 2003; Carnaval and Moritz, 2008; Saillard *et al.*, 2009; Miloslavich *et al.*, 2011). Therefore, South American coastal flora shows a peculiar diversity with a range of biogeographical processes involving different population demographic processes (Silva *et al.*, 2018; Massante and Gerhold, 2020). Although the studies on plant diversification in South America have received increased attention in the last years, analyses focusing the post-glacial re-colonization, speciation, migration, and colonization of coastal areas are still scarce (Sérsic *et al.*, 2011; Turchetto-Zolet *et al.*, 2013; Leal *et al.*, 2016).

The species' geographical distribution and genetic diversity result from historical and contemporary processes acting together with ecological factors (Loveless and Hamrick, 1984; Huang *et al.*, 2016; Schierenbeck, 2017). The multiple environmental particularities in the coastal areas constitute exciting models for studying genetic differentiation in response to climate changes, physical barriers, and ecological features (Kadereit and Westberg, 2007; Escudero *et al.*, 2010; Sork, 2016). Coastal regions have common characteristics, such as intrinsic linear distributions, high salinity, wind strength, and tidal influence, that investigate convergent demographic patterns among species from different areas (Escudero *et al.*, 2010). The colonization and the genetic isolation are critical events in the evolutionary dynamics of coastal plant populations (Thompson, 1999), mainly because the spread to new environments generates signals on the genetic diversity and structure of species (Excoffier *et al.*, 2009).

The geographical distance and environmental differences influence the genetic differentiation across species range because they affect the genetic variation and structure between populations (Manel *et al.*, 2003; Nosil *et al.*, 2009; Lee and Mitchell-Olds, 2011).

Analyses such as the isolation-by-distance (IBD) and isolation-by-environment (IBE) can identify the causes of the genetic differentiation resulting from geographic distance and interactions between organisms and their environments, respectively (Orsini *et al.*, 2013; Sexton *et al.*, 2014; Wang and Bradburd, 2014).

Some studies have indicated that the differences in micro-environments or resulting from abiotic factors (temperature and superficial marine currents) may promote differential selection that limits the establishment of species (e.g., Tellier *et al.*, 2009, 2011; Mori *et al.*, 2015; Francisco *et al.*, 2018). Despite that, the evaluation of the relative influence of space and environment on the genetic differentiation in South American coastal plains is still scarce (Baranzelli *et al.*, 2014; Silva-Arias *et al.*, 2017; Meireles and Manos, 2018).

The South Atlantic coastal Plain (SACP) is a flat, continuous, and open region constituting the most extensive coastal region in South America. The SACP extends NE-SW for approximately 600 km, occupied mostly by large coastal lakes, and crossed by two perennial water channels (Tomazelli *et al.*, 2000; Weschenfelder *et al.*, 2010). The SACP gradually arose during sea-level transgressions and regressions processes caused by glacial-interglacial cycles during the last 400 thousand years. The most substantial transgression and regression cycles let the formation of four main sand barriers to be positioned parallel to the coastline (barrier-lagoon systems I to IV; Tomazelli *et al.*, 2000; Tomazelli and Dillenburg, 2007). The harsh environment, such as strong spring-summer sea breezes from the northeast and high insolation, strongly influences this region such as strong spring-summer sea breezes from the northeast and high insolation (Dillenburg *et al.*, 2009), which was responsible for the current topography and, consequently, influenced the distribution and variability of genetic lineages in contemporary plants (e.g., Mäder *et al.*, 2013; Ramos-Fregonezi *et al.*, 2015; Silva-Arias *et al.*, 2017).

In this study, we aimed to investigate the historical and contemporary processes involved in the diversification of coastal plants in South America. We examined potential topographical and climatic predictors for population structure and gene flow during the colonization of the SACP based on a small shrub, perennial, and coastal nightshade species, *Calibrachoa heterophylla*. Our results provided information that can support the establishment of general scenarios describing evolutionary processes for plants from the coastal regions in South America and addressing conservation gaps in the face of climate changes.

MATERIALS AND METHODS

Study system

The species of *Calibrachoa* (Solanaceae) occur in subtropical and temperate grasslands in southern Brazil, northeast Argentina, and Uruguay. The genus encompasses ca. 30 species, among which *C. heterophylla* is the only species that colonized coastal environments (Mäder and Freitas, 2019). This species is diploid (2n = 18), semi-prostrated, and displays purplish bee-pollinated flowers; the fruits are capsules and produce dozens of tiny seeds (< 1.4 mm) with no dispersal mechanisms. The species occupies open sandy grasslands, dunes, or rocky outcrops in lakeside or marine environments from ~ 28 Lat S to 32 Lat S in the SACP (Mäder *et al.*, 2013). Longitudinally, populations of *C. heterophylla* occur from the seashore to less than 90 km from the coast, with the populations separated from the sea by big lagoons. Just one disjointed and small group of populations (Fig. 1A) can be found outside from SACP, restricted to the sandbanks alongside the Santa Maria River basin, ~ 55 Long W.

The phylogeographic structure of *C. heterophylla* reveals one inland and three coastal intra-specific plastid DNA (cpDNA) lineages that likely resulted from divergence before the SACP formation. Two river channels acted as paleo-barriers, splitting the coastal lineages

(Mäder *et al.*, 2013). The current distribution of *C. heterophylla* in SACP could be shaped through a population expansion following the last marine regression (Mäder and Freitas, 2019), ca. 7-8 thousand years ago (kya; Tomazzeli *et al.*, 2000).

Sample collections

We sampled a total of 253 individuals from 15 locations (hereafter called populations; Fig. 1A) that covered the entire *C. heterophylla* known distribution. We collected leaves of all individuals found in each locality and preserved them in silica gel. The number of individuals per population varied from three to 41 (Table 1).

Laboratory procedures

The total DNA was extracted following a CTAB-based protocol (Roy *et al.*,1992) and amplified for ten anonymous microsatellite loci (Che18, Che59, Che119, Che26, Che34, Che81, Che82, Che85, Che72, and Che126) developed for *C. heterophylla*, following standard protocols for PCR and genotyping procedures (Silva-Arias *et al.*, 2015).

Characterization of the genetic diversity

We performed tests for linkage disequilibrium and deviations from Hardy-Weinberg equilibrium (HWE) within each population for each locus. We assessed the significance of HWE deviations using 10^6 Markov chain steps and Fisher's exact probability tests in ARLEQUIN 3.5 (Excoffier and Lischer, 2010). We estimated the genetic diversity based on average rarefied allelic richness, private alleles, observed heterozygosity (H_O), expected heterozygosity (H_E), the Garza-Williamson (G-W) index, and inbreeding coefficient (F_{IS}; with confidence limits from 1000 bootstrap resampling over loci) using the POPPR 2.8.5 (Kamvar

126 *et al.*, 2014, 2015) and HIERFSTAT 0.04-22 (Goudet, 2005, 2014) in R 3.6.3 package (R Core
127 Team, 2019), and ARLEQUIN.
128
129 *Genetic structure*
130 We assessed the genetic structure employing two model-based clustering methods and two
131 exploratory data analyses (François and Waits, 2016). The model-based clustering methods
132 used were STRUCTURE 2.3.4 (Pritchard *et al.*, 2000) and the spatial Bayesian clustering
133 program TESS 2.3. These analyses provide estimates for the number of genetic clusters (K) in
134 HWE equilibrium, individual assignment probabilities, and compute the proportion of the
135 genome of each individual that can be assigned to the inferred clusters.
136 For STRUCTURE analysis, the number of clusters evaluated ranged from 1 to the total
137 number of populations (15), with ten independent runs per K-value. We performed each run
138 using 2.5×10^5 burn-in periods and 1.0×10^6 Markov chain Monte Carlo repetitions after the
139 burn-in, under an admixture model, assuming correlated allele frequencies (Falush *et al.*,
140 2003), and including a priori sampling locations as prior (*locprior*) to detect weak population
141 structure. The *locprior* option is not biased toward detecting structure when it is not present
142 and can improve the STRUCTURE results when implemented with few loci (Hubisz *et al.*,
143 2009). To obtain the K value that better explains the structure based on the genetic dataset, we
144 assessed the measures of the ΔK method (Evanno *et al.*, 2005) that is useful to recover the
145 highest level of genetic structure.
146 TESS implements a spatial assignment approach to group individuals into clusters
147 accounting for samples' geographical locations, giving them higher probabilities of belonging
148 to the same genetic cluster to those that are spatially closer in the connection network. For
149 TESS, we ran100 000 generations, with 50 000 generations as the burn-in, using the
150 conditional autoregressive (CAR) admixture model, and starting from a neighbour-joining

tree. We ran 20 iterations for each value of maxK ranging from 2 to 15. We added small perturbations to the original spatial with a standard deviation equal to 0.2 to obtain single different coordinates for each individual, because of the spatial proximity among individuals from each collection site allowed to obtain only one coordinate. We assessed the convergence inspecting the post-run log-likelihood plots and obtained the support for alternative K values inspecting the statistical measure of the model prediction capability from deviance information criterion (DIC; Spiegelhalter *et al.*, 2002). We computed and plotted the average of DIC values to detect maxK value at the beginning of a plateau. Replicated runs of best K results for both STRUCTURE and TESS were summarized and plotted with the POPHELPER (Francis, 2017) R package.

Additionally, to detect genetic structure, we implemented two exploratory data analyses multivariate method (François and Waits, 2016), the Discriminant Analysis of Principal Components (DAPC; Jombart *et al.*, 2010) and the spatial Principal Component Analysis (sPCA; Jombart *et al.*, 2008), both using the ADEGENET 2.1.3 (Jombart, 2008) R package. For the DAPC analysis, the SSR data were first transformed using Principal Component Analysis and keeping all principal components (PCs). After that, we implemented the function *find.clusters* to obtain the optimal number of clusters that maximizes the between-group variability using the lowest Bayesian Information Criterion (BIC) score. To avoid overfitting, we set an optimal reduced number of PCs to retain given the best number of clusters using the function *optim.a.score*. Finally, the DAPC was implemented with the number of clusters and PCs to the optimal values and plotted a scatter plot of the two first components with the function *s.class*.

sPCA of genetic structure incorporates spatial information to maximize the product of spatial autocorrelation (Moran's I) and the variance for each eigenvector, which produces orthogonal axes that describe spatial patterns of genetic variation. The spatial information is

included in the analysis using a spatial weighting matrix derived from a connection network. To test the effect of the neighbouring definition on the results, we ran the sPCA using six different connection networks available in the function *chooseCN*. For these analyses, we used the same perturbed coordinates used in TESS analysis. Monte Carlo simulations (global and local tests) were used with 10 000 permutations to test for non-random spatial association of population allele frequencies for all sPCA implemented.

Historical and contemporary gene flow estimations

Contemporary asymmetric migration rates were estimated using a Bayesian approach implemented in BAYESASS 3.0 (Wilson and Rannala, 2003). We ran 10^8 iterations and a burn-in of 10^7. We adjusted the mixing of allele frequencies, inbreeding coefficients, and migration rates parameters to 0.6, 0.6, and 0.3, respectively, to obtain acceptance rates around 40%. We assessed convergence examining the log-probability plots and the effective sample sizes for each run using TRACER 1.6 (Rambaut *et al.,* 2014) and looking for consistency of the migration estimates among three independent runs with different initial seed numbers.

We assessed historical gene flow testing the support of four alternative scenarios given our genetic dataset using Bayes factors calculated from the marginal likelihood approximations (Beerli and Palczewski, 2010). We used the coalescent-based MIGRATE-N 3.2.6 (Beerli and Felsenstein, 2001) software to estimate the mutation-scaled population size (Θ) and a mutation-scaled migration (M) parameter. To assess the support of each migration model, we used the Bézier log-marginal likelihood approximations.

For all models, we pooled the populations into four groups according to the geographical distribution and genetic structure (see Results Figs. 1A and 2). The ‘Inland’ group included the São Francisco de Assis, Cacequi 1, and Cacequi 2 populations; ‘West’ group encompassed the Arambaré, Barra do Ribeiro, and Pelotas populations; ‘North’ included the

Santo Antônio da Patrulha, Torres, and Laguna populations; and 'South' group clustered the Mostardas 1, Mostardas 2, São José do Norte 1, São José do Norte 2, Rio Grande, and Santa Vitória do Palmar populations.

We evaluated four migration models: (1) source-sink from inland with unidirectional migration from 'Inland' group to the remaining groups; (2) source-sink from the west with unidirectional migration from 'West' group to the remaining groups; (3) step-stone from inland with unidirectional migration from Inland to West and from West to North and South; and (4) step-stone from the coast with unidirectional migration from North to West, from South to West, and from West to Inland (Supplementary Data Fig. S1).

We ran the MIGRATE-N Bayesian inference in the Cipres Science Gateway 3.3 (Miller *et al.*, 2010), with one long chain of 5×10^6 steps, sampling at every 100^{th} increment, and a burn-in of 3×10^4 steps. We used uniform priors and slice sampling for both Θ and M ranging from 0 to 20 (mean = 10, delta = 0.5). We used a heating scheme (Metropolis-coupled Markov Chain Monte Carlo) with four parallel chains and temperatures of 1, 1.5, 3, and 10^6.

Space, topography, environment, and genetic differentiation

Spatial correlation patterns under isolation-by-distance (IBD) arouse bias in several genetic structure tests (Frantz *et al.*, 2009; Meirmans, 2012). Therefore, we assessed the IBD through linear regression of linearized pairwise F_{ST} genetic distances and log-transformed geographical distances (Rousset, 1997) using a Mantel test, assessing the significance with 10 000 randomizations in VEGAN 2.5-6 (Oksanen *et al.*, 2015) R package.

We calculated the pairwise F_{ST} (Weir and Cockerham, 1984) matrix with the HIERFSTAT package. We obtained the geographical inter-population distance matrix calculating the linear Euclidean distance between X and Y UTM 22S (reference EPSG: 32722) populations'

coordinates transformed from Long/Lat coordinates with RGDAL 1.0-4 (Bivand *et al.*, 2015) R package.

We tested isolation-by-environment (IBE) models to examine whether differences in climatic conditions explain the observed inter-population genetic differentiation in *C. heterophylla*. We calculated the climatic dissimilarity matrices between each populations' pair for the following bioclimatic variables: total annual precipitation, total annual days with rain, precipitation seasonality, mean annual temperature, mean summer maximum temperature, mean winter minimum temperature, mean temperature range, and temperature seasonality. We took the values of those climatic variables from raster layers specifically developed for the SACP derived from a high-density sampling of climate stations throughout the region, geostatistical modelling, and spatial interpolation (Silva-Arias *et al.*, 2017).

Considering that strong summer winds in the SACP can be an important vector for seed or vegetative propagules movement, we also included a wind connectivity matrix in the IBE tests. We calculated surface wind direction and speed data for southern Hemisphere's spring months (September to November) 2011–2016 sampled every three hours. We downloaded the data from the Global Forecasting System using the RWIND 1.1.5 (Fernández-López and Schliep, 2019) R package. For each sampled time, we transformed direction and speed values into raster layers using the *wind2raster* function to obtain transition layers using the function *flow.dispersion*. Finally, we calculated pairwise cost distance matrices with the function *costDistance* in GDISTANCE 1.3-1 (van Etten, 2017) R package. We then averaged the matrices for all-time series. We plotted the final matrix with the QGRAPH 1.6.5 (Epskamp *et al.*, 2012) in the R package.

To test for possible models of inter-population differentiation linked to landscape discontinuities alongside the SACP, we extended the IBD and IBE analyses using raster grids. We outlined two coast distance models (Supplementary Data Fig. S2): (1) the *continuous* (or

null) model wherein no landscape discontinuity affects the inter-population connectivity. We created a raster grid with all cells values equal to 1, including all cells on freshwater surfaces. This model is expected to resemble a Euclidean geographical distance, but it is more proper for comparisons with models based on circuit theory; and (2) the *water bodies* model, which proposes that the widespread freshwater bodies in the SACP restrict the connectivity between populations. For that, we created a raster grid with all land cells values equal to 1, and cells within freshwater surfaces as complete barriers (*no data*). We generated pairwise cost distance matrices using the function *transition* in GDISTANCE package considering an eight-neighbour cell connection scheme, Long/Lat coordinates per population as nodes, and raster resolution of 0.09 degrees (~ 10 km).

We examined the relationships between genetic differentiation (F_{ST}) and geographical or topographical distances (IBD) and environmental dissimilarity (IBE) using multiple matrix regressions with randomization (MMRR; Wang, 2013) implemented in R.

RESULTS

Genetic diversity

We found a total of 140 alleles across the ten microsatellite loci. The mean number of alleles per locus was 14, ranging from seven (Che59) to 17 (Che81). All loci showed higher H_e (Supplementary Data Fig. S3) with 25% of the locus-population combinations showing a departure of HWE ($P < 0.05$). We detected a significant linkage disequilibrium signal ($P < 0.01$) for several loci pairs, but as the linkage pattern was not consistent across populations for any loci pair, we assumed linkage equilibrium and maintained all loci in the analyses. MICROCHECKER analysis did not show null alleles, scoring errors, or stutter peaks for any locus.

Populations located outside of SACP and those collected at the west side of the Patos Lagoon showed higher genetic diversity overall loci (Fig. 1B). In contrast, the coastal populations located at the northern and southern edges of species distribution in SACP (Laguna and Santa Vitória do Palmar populations, respectively) had lower genetic diversity values. Average values across loci for H_o ranged from 0.72 (São Francisco de Assis) to 0.31 (Laguna) and for H_e from 0.74 (Cacequi 2) to 0.48 (São José do Norte 1). We found 22% of the alleles being exclusive to one population, with Barra do Ribeiro showing the highest number of private alleles (eight), whereas Pelotas, Mostardas 1, São José do Norte 1, and São José do Norte 2 populations had no private alleles. Garza-Williamson values ranged from 0.39 (Cacequi 1) to 0.83 (Torres). We found positive and significant inbreeding coefficients (F_{IS}) for five populations (Fig. 1B), all of them located at the borders (northern and southern) of species' distribution in the SACP (Fig. 1A; Table 1).

Genetic structure

The best K value inferred from the ΔK method in STRUCTURE analysis was K = 4 (Supplementary Data Fig. S4A), whereas the curve of average DIC values obtained with TESS analyses showed a plateau after maxK = 8 and maxK = 2, 3, and 4 runs had the lowest standard deviations (Supplementary Data Fig. S4B). Accounting for these results, we analysed the bar plots of membership probability from K = 2 to K = 8.

The recovered population structure had a strong geographic signal. Genetic clustering obtained with STRUCTURE (Fig. 2) and TESS (Supplementary Data Fig. S5) showed similar results. For both approaches, assignment probabilities obtained for K = 2 delimited one cluster composed of populations located at northern SACP and a second group composed by remain populations. When K = 3, one group encompassed the northern coastal populations, the second clustered the southern coastal populations, and the third brought together all

299 populations located on the west side of the Patos Lagoon and the three inland populations.
300 Higher values of K showed differences between the two Bayesian clustering methods in the
301 sequence that groups were incorporated; however, both recovered the same clustering pattern
302 at K = 8. With this K, the first group was composed by the three inland populations; the
303 second and third groups encompassed solely a single population each (Barra do Ribeiro and
304 Pelotas, respectively, both located on the west of Patos Lagoon); the forth cluster grouped two
305 populations from the northern SACP (Santo Antonio da Patrulha and Torres); the fifth cluster
306 encompassed the individuals from Laguna population (the northernmost distributed
307 population); the sixth cluster grouped São José do Norte 1 and São José do Norte 2
308 populations; the seventh cluster enclosed the individuals from the southernmost located
309 population (Santa Vitória do Palmar); and the eighth group was not preferentially linked to
310 any population, instead showed low membership probabilities for individuals from several
311 populations.

312 We found higher admixed membership for individuals from populations located in
313 geographical transitional regions (Fig. 2 and Supplementary Data Fig. S5). The most notable
314 cases were Mostardas 1 and Mostardas 2 populations located between the north and south
315 SACP portions, with all individuals from these populations showing membership probability
316 assigned into all clusters except the inland group. Individuals from the Rio Grande population
317 also showed high mixed membership and achieved some discrepancy between the two
318 Bayesian assignment tests. For the individuals from the Rio Grande population, STRUCTURE
319 assigned around 60% of the membership to the Torres genetic component, while TESS
320 supported a higher membership probability to the Santa Vitória do Palmar component.

321 Exploratory analyses revealed similar results to the Bayesian clustering analyses.
322 Although the lowest BIC score was for K = 8 (Supplementary Data Fig. S6), DAPC
323 scatterplot of the two main discriminant components (Fig. 1C) revealed three main groups,

delimiting northern and southern coastal populations in two different groups, and a third group encompassing individuals from inland, Patos Lagoon western side, and the two Mostardas populations. sPCA (Fig. 1D) recovered the two main groups formed by the northern and southern edge coastal populations on the first sPC axis. The Torres and Santo Antônio de Patrulha from the northern and Santa Vitória do Palmar from the southern occupied opposed spaces related to their respective groups on the first sPC axis, while the remaining populations showed a gradient of differentiation on the second sPC axis.

Migration rates

The mean migration rate, as estimated with BAYESASS, was 0.015. However, the vast majority of the pairwise population estimations showed relatively wide confidence intervals ranging between 0 and 0.1, with only four population pairs showing higher posterior effective migration rates and confidence intervals above zero. Among these four cases, the most outstanding was Mostardas2 to Arambaré ($N_m \approx 0.08$; 95% CI 0.01 - 0.14) that supports migration between populations separated by the Patos Lagoon. The other three cases involved neighbour populations, Cacequi1 to Cacequi2 ($N_m \approx 0.12$; 95% CI 0.05-0.19), Mostardas2 to Mostardas1 ($N_m \approx 0.07$; 95% CI 0.01-0.13), and SJoséNorte2 to SJoséNorte1 ($N_m \approx 0.16$; 95% CI 0.09-0.22). Migration estimates obtained from independent runs of BAYESASS showed similar values (Supplementary Data Table. S1).

The model-based coalescent approach implemented in MIGRATE-N supported the *step-stone from the coast* as the most likely historical migration model between population groups (Table 2, Supplementary Data Fig. S1C). Parameter estimation taken from the best-supported model showed that 'Inland' group had the highest mean mutation scaled population size (Θ), which was around eight times higher than the Θ estimated for 'West' and 'North' groups, and around of 20 times higher than the Θ estimated for 'South' group that showed the lowest

value (Table 2). Migration from 'West' to 'Inland' had the highest mean mutation scaled migration rate that was twice higher than the 'North' to 'West' and five times when compared to the 'South' to 'West' values (Table 2).

Isolation-by-distance, isolation-by-environment, and resistance tests

Measures of population differentiation (Fig. 3A) F_{ST} ranged from 0.01 between Mostardas1 and Mostardas2 populations to 0.54 between Laguna and São José do Norte1 populations. Linear regressions showed a significant positive relationship between genetic (Fig. 3A) and linear geographical (Fig. 3B) distances ($R^2 = 0.14$; $P < 0.001$) supporting a IBD pattern for the data set (Fig. 4A). Mantel test also supported a correlation between the genetic and geographical distance matrices (Mantel's $r = 0.38$, $P < 0.001$).

Analyses testing the relationship among geographical distance, climate variables, and genetic differentiation based on MMRR approach showed significant association between the genetic dissimilarity and Euclidean distance ($R^2 = 0.21$, $\beta = 1.7 \times 10^{-7}$, $P < 0.001$) when regressed with F_{ST} as the unique explanatory variable. MMRR models implemented with each of the assessed climate variables and Euclidean distance as explanatory variables showed significant relationship only for precipitation seasonality (Fig. 3C; $R^2 = 0.35$, $P = 0.003$; $\beta_{precseason} = 7.5 \times 10^{-3}$, $P = 0.05$; $\beta_{Euc} = 1.1 \times 10^{-7}$, $P = 0.02$, respectively). IBD tests based on topographic models based on coast distances showed that the *continuous* model (i.e., landscape matrix with no topographic discontinuities; Supplementary Data Fig. S2A) explained slightly better the genetic differentiation (F_{ST}; $R^2 = 0.16$, $\beta = 0.022$, $P = 0.006$) than the *water bodies* ($R^2 = 0.14$, $\beta = 0.02$, $P = 0.011$) model (i.e., landscape matrix with water bodies as full barriers to population connectivity; Supplementary Data Fig. S2B). The wind connectivity matrix (Figs. 4B and 4C) showed a consistent north-to-south asymmetric step-stone pattern where marginal populations appeared strongly isolated. Moreover, populations

374 located at the west side of the Patos Lagoon became receptors from coastline populations. The
375 coast distance wind matrix (Fig. 4A) showed significant correlation with the F_{ST} genetic
376 distance matrix ($R^2 = 0.19$, $\beta = 0.001$, $P = 0.0037$).
377

378 **DISCUSSION**

379 In this study, we analysed patterns of genetic diversity and structure of *Calibrachoa*
380 *heterophylla* to infer the influence of topographical and environmental features on the gene
381 flow during the recent colonization of a coastal plain in South America.
382 Our results provided consistent evidence for limited and asymmetric gene flow, mainly
383 limited by the geographical distance. The populations from northern and southern edges of
384 the species distribution showed negligible historical and contemporary immigration rates
385 probably related with an isolation-by-environment through the precipitation conditions. We
386 also found that the more outstanding topographical feature in the South Atlantic Coastal Plain
387 (the big water bodies) does not seem to constrain *C. heterophylla* populations' gene flow.
388

389 *Historical and contemporary drivers of genetic structure in Calibrachoa heterophylla*
390 There is a hierarchical pattern of genetic structure related to both historical and contemporary
391 landscape features. The highest level of population structure showed three well-supported
392 groups, northern, central, and southern groups. The central group also included the inland
393 populations. This main clustering pattern mirrors the phylogeographical structure of *C.*
394 *heterophylla* based on cpDNA (Mäder *et al.*, 2013). The retention of historical signals of
395 genetic structure in highly variable markers, such as microsatellites, is expected for studies
396 involving the entire geographic range of species, which reinforces the importance of
397 considering the historical patterns for landscape genetic approaches (Anderson *et al.*, 2010).
398 The populations from the intersection between northern and southern regions, such as

399 Mostardas 1 and Mostardas 2 populations, or those between west Patos Lagoon and southern
400 regions, as Pelotas population, had higher admixture values to a secondary gene flow between
401 previously differentiated intraspecific lineages (Fig 1).

402 The influence of geographical distances on the genetic structure was evident in several
403 levels of *C. heterophylla* genetic structure. The northern, southern, and central groups showed
404 a main latitudinal pattern of structure. At a fine scale, we found that individuals from
405 peripheral populations conformed independent groups with individuals' membership higher
406 than 80%, as seen in Santa Vitória do Palmar, inland populations São Francisco de Assis,
407 Cacequi 1, and Cacequi 2, and Laguna locations (Figs. 1 and 2; Supplementary Data Fig. S3).
408 Genetic drift due to strong geographical isolation (Whigham *et al.,* 2008) can explain
409 individuals' assignment to a completely separated group.

410 We observed few departures from the geographical frame in the genetic structure in
411 some distant populations for which the assignment tests suggested as sharing partial genetic
412 identities, such as Laguna and São José do Norte and Torres and Rio Grande population pairs.
413 In both cases, populations from northern and southern SACP regions were involved. Either
414 persistent ancestral variation after population divergence or randomly driven processes, such
415 as the fixation of the same allele during an expansion wave (Excoffier and Ray, 2008) or
416 homoplasy (Grimaldi and Crouau-Roy, 1997; van Oppen *et al.,* 2000; Schaal and Olsen,
417 2000) could equally explain that partial genetic affinity between spatially distant populations.
418 A long-distance gene flow seems an unlikely scenario based on the high F_{ST} between these
419 populations and the observed low migration rates.

420 The Pelotas population showed several different results according to the methodology
421 and structure level inferred. Exploratory and STRUCTURE analyses grouped Pelotas with the
422 inland populations (Figs. 1 and 2), while TESS suggested that Pelotas would be more related
423 to the southern group (Supplementary Data Fig. S3). Similarly, a population fine structure

patterns (i.e., K = 5-8) for both STRUCTURE and TESS suggested a higher affinity of Pelotas population with São José do Norte or forming an independent group with all individuals assigned at ~ 100% of membership probability (Fig. 2, Supplementary Data Fig. S3). The geographic position of Pelotas population and environmental features could have drawn this scenario. Regarding the geographic position, the Pelotas population is located close to the southern coastal populations, such as the Rio Grande and São José do Norte. However, the Patos Lagoon separates the Pelotas population from the seashore, which can lead Pelotas to receive migrants from coastal populations in a more continental environment. Nevertheless, inter-annual rainfall conditions, as well as the continental-scale periodic climatic fluctuations, such as El Niño, can also affect the fluvial discharge and the wind responsible for the salinization and desalination processes in the Patos Lagoon (Möller *et al.,* 1996, 2001; Möller and Castaing, 1999). This environmental dynamic could continuously change the individuals' establishment or survival rates, with the coastal or continental gene pools probably leading to a differential genetic profile.

Patos Lagoon development let to a secondary contact between previously diverged lineages

The populations located close to the Patos Lagoon, Arambaré, Mostardas 1, Mostardas 2, São José do Norte 1, São José do Norte 2, and Rio Grande (Fig. 1A) showed the highest levels of genetic admixture (Fig. 2; Supplementary Data Fig. S3) and the lowest F_{ST} values (Fig. 3A) among the coastal populations. These results could be related to the recent geomorphological history of the SAPC region. During most of the Quaternary Period, two rivers (Jacuí and Camaquã rivers), including several channels corresponding to their temporal dynamic delta systems, crossed the Patos Lagoon (Weschenfelder *et al.,* 2014). After the formation of the barrier systems III and IV, the two most recent ocean regressive-transgressive events, the Patos Lagoon was completely close by sands from the inlets (Santos-Fischer *et al.*, 2016),

449 which could have constituted an obstacle for the establishment of the population in the east
450 side of the lagoon. In contrast, the northern and southern regions, which correspond to the
451 well-established barrier systems I and II (cf. Fig. 1 in Tomazelli and Dillenburg, 2007), could
452 let to the establishment and differentiation of main coastal lineages that, later, spread and
453 experienced a secondary contact on the east side of the Patos Lagoon generating the current
454 patterns of genetic admixture in this region. This recent admixture processes can also explain
455 the lack of private alleles in Pelotas, São José do Norte 1, São José do Norte 2, and Mostardas
456 1 populations (Fig. 1B).

457 The east side of Patos Lagoon (seashore side) has the strongest wind influence within
458 the SACP (Fig. 4B; Martinho *et al.*, 2010) that can increase the seed dispersal alongside the
459 region generating, in consequence, higher admixture rates. The gene flow estimations among
460 *C. heterophylla* populations support an asymmetric migration from coastal to inland locations,
461 even at great distances crossing the coastal lakes (Figs. 1 and 4). Despite the differences in the
462 intraspecific divergence history between *C. heterophylla* (Mäder *et al.*, 2013) and the co-
463 distributed *P. integrifolia* subsp. *depauperata* (Ramos-Fregonezi *et al.*, 2015), both taxa
464 shared the same pattern of high genetic admixture based on microsatellite data in populations
465 located at the east of Patos Lagoon (Silva-Arias *et al.*, 2017). This congruent pattern between
466 species indicates that the current and historical dynamics in the topographical and
467 environmental conditions in SACP are responsible for the admixture patterns and the genetic
468 structure in this region.

469 The precipitation seasonality is different between the northern and southern extremes
470 of SACP (Fig. 3C), and there is a significant positive relationship between this environment
471 feature and genetic differentiation. Moreover, the immigration for the SAPC edges falls
472 within the lowest estimates (Supplementary Data Fig. S5). Altogether, these results point to a
473 genetic divergence process enhanced by differential rainfall regimes alongside SACP. The

474 strong correlation between precipitation seasonality and genetic differentiation was also found
475 for the coastal populations of *Petunia integrifolia* subsp. *depauperata* (Silva-Arias *et al.*,
476 2017). Ecological differentiation can promote selection against immigrants that leads, in a
477 genome-wide context, to a reduction of gene flow, reproductive isolation, and enhances the
478 stochastic effects of genetic drift (Hendry, 2004; Nosil *et al.*, 2005, 2009). For *C.*
479 *heterophylla*, the limited migration rates from the central to marginal distribution could
480 enhance the fixation of locally adaptive alleles in peripheral populations by preventing the
481 gene swamping (Alleaume-Benharira *et al.*, 2006).

482 We found that both geomorphological and environmental conditions influenced population
483 demographic processes in coastal plants, such as differentiation, connectivity, and local
484 adaptation. The main current population differentiation in *Calibrachoa heterophylla* is
485 determined by historical processes and the age of the deposition of the coastal plain. In
486 contrast, population connectivity is mainly determined by geographic distance and wind fields
487 but seems to be not affected by significant barriers like water bodies. Besides, marginal
488 populations appear to present local differentiation related to rainfall conditions.

489

490 **ACKNOWLEDGEMENTS**

491 The authors thank to G. Mäder for help in fieldwork and J.R Stehmann for plant
492 identification. G.A.S.-A. and L.B.F. designed the study; G.A.S.-A. performed fieldwork,
493 laboratory experiments, analysed data, and interpreted the results; G.A.S.-A. and L.C.-V.
494 discussed the results and wrote the manuscript. G.C.G. performed laboratory genotyping;
495 L.B.F. supervised the project and provided resources for the research. All authors reviewed
496 the manuscript. All authors declare no conflict of interest. All data underlying the study are
497 included in the manuscript or its supplementary materials.

498

FUNDING

This work was supported by the Conselho Nacional de Desenvolvimento Científico e Tecnológico (CNPq), Coordenação de Aperfeiçoamento de Pessoal de Nível Superior (CAPES), and Programa de Pós-Graduação em Genética e Biologia Molecular da Universidade Federal do Rio Grande do Sul (PPGBM-UFRGS). G.A.S.-A. was supported by a scholarship from the Francisco José Caldas Institute for the Development of Science and Technology (COLCIENCIAS).

LITERATURE CITED

Alleaume-Benharira M, Pen IR, Ronce O. 2006. Geographical patterns of adaptation within a species' range: interactions between drift and gene flow. *Journal of Evolutionary Biology* **19**: 203–215.

Anderson CD, Epperson BK, Fortin M-J, *et al.* 2010. Considering spatial and temporal scale in landscape-genetic studies of gene flow. *Molecular Ecology* **19**: 3565–3575.

Baranzelli MC, Johnson LA, Cosacov A, Sérsic AN. 2014. Historical and ecological divergence among populations of *Monttea chilensis* (Plantaginaceae), an endemic endangered shrub bordering the Atacama Desert, Chile. *Evolutionary Ecology* **28**: 751–774.

Beerli P, Felsenstein J. 2001. Maximum likelihood estimation of a migration matrix and effective population sizes in n subpopulations by using a coalescent approach. *Proceedings of the National Academy of Sciences USA* **98**: 4563–4568.

Beerli P, Palczewski M. 2010. Unified framework to evaluate panmixia and migration direction among multiple sampling locations. *Genetics* **185**: 313–326.

Behling H. 2003. Late glacial and Holocene vegetation, climate and fire history inferred from Lagoa Nova in the southeastern Brazilian lowland. *Vegetation History and*

Archaeobotany **12**: 263–270.

Bivand R, Keitt T, Rowlingson B. 2015. rgdal: Bindings for the 'Geospatial' data abstraction library. https://cran.r-project.org/package=rgdal.

Carnaval AC, Moritz C. 2008. Historical climate modelling predicts patterns of current biodiversity in the Brazilian Atlantic forest. *Journal of Biogeography* **35**: 1187–1201.

Dillenburg SR, Barboza EG, Tomazelli LJ, Ayup-Zouain RN, Hesp PA, Clerot LCP. 2009. The Holocene coastal barriers of Rio Grande do Sul. In: *Geology and Geomorphology of Holocene Coastal Barriers of Brazil*. Lecture Notes in Earth Sciences, vol. 107. Berlin:Springer, 53-91.

Epskamp S, Cramer AOJ, Waldorp LJ, Schmittmann VD, Borsboom D. 2012. *qgraph*: network visualization of relationships in psychometric data. *Journal of Statistical Software* **48**: 1-18.

Escudero M, Vargas P, Arens P, Ouborg NJ, Luceño M. 2010. The east-west-north colonization history of the Mediterranean and Europe by the coastal plant *Carex extensa* (Cyperaceae). *Molecular Ecology* **19**: 352–370.

van Etten J. 2017. *R* Package gdistance: distances and routes on geographical grids. *Journal of Statistical Software* **76**: 1-21.

Evanno G, Regnaut S, Goudet J. 2005. Detecting the number of clusters of individuals using the software structure: a simulation study. *Molecular Ecology* **14**: 2611–2620.

Excoffier L, Lischer HEL. 2010. *Arlequin* suite ver 3.5: a new series of programs to perform population genetics analyses under Linux and Windows. *Molecular Ecology Resources* **10**: 564–567.

Excoffier L, Ray N. 2008. Surfing during population expansions promotes genetic revolutions and structuration. *Trends in Ecology & Evolution* **23**: 347–351.

Excoffier L, Foll M, Petit RJ. 2009. Genetic consequences of range expansions. *Annual*

549 *Review of Ecology, Evolution, and Systematics* **40**: 481–501.

550 **Falush D, Stephens M, Pritchard JK. 2003.** Inference of population structure using
551 multilocus genotype data: linked loci and correlated allele frequencies. *Genetics* **164**:
552 1567–1587.

553 **Fernández-López J, Schliep K. 2019.** *rWind*: download, edit and include wind data in
554 ecological and evolutionary analysis. *Ecography* **42**: 804–810.

555 **Francis RM. 2017.** *POPHELPER*: an R package and web app to analyse and visualize
556 population structure. *Molecular Ecology Resources* **17**: 27–32.

557 **Francisco PM, Mori GM, Alves FM, Tambarussi EV, Souza AP. 2018.** Population genetic
558 structure, introgression, and hybridization in the genus *Rhizophora* along the Brazilian
559 coast. *Ecology and Evolution* **8**: 3491–3504.

560 **François O, Waits LP. 2016.** Clustering and assignment methods in landscape genetics. In
561 Balkenhol N, Cushman SA, Storfer AT, Waits LP, eds. *Landscape genetics: concepts,*
562 *methods, applications.* Chichester: Wiley, 114-128.

563 **Frantz AC, Cellina S, Krier A, Schley L, Burke T. 2009.** Using spatial Bayesian methods
564 to determine the genetic structure of a continuously distributed population: clusters or
565 isolation by distance? *Journal of Applied Ecology* **46**: 493–505.

566 **Goudet J. 2005.** *hierfstat*, a package for R to compute and test hierarchical F-statistics.
567 *Molecular Ecology Notes* **5**: 184–186.

568 **Goudet J. 2014.** *hierfstat*: estimation and tests of hierarchical F-statistics. R package version
569 0.04-14. http://CRAN.R-project.org/package=hierfstat.

570 **Grimaldi M-C, Crouau-Roy B. 1997.** Microsatellite allelic homoplasy due to variable
571 flanking sequences. *Journal of Molecular Evolution* **44**: 336–340.

572 **Hendry AP. 2004.** Selection against migrants contributes to the rapid evolution of
573 ecologically dependent reproductive isolation. *Evolutionary Ecology Research* **6**: 1219–

1236.

Hickerson MJ, Carstens BC, Cavender-Bares J, *et al.* 2010. Phylogeography's past, present, and future: 10 years after Avise, 2000. *Molecular Phylogenetics and Evolution* **54**: 291–301.

Huang W, Zhao H, Zhao X, Li Y, Lian J. 2016. Effects of environmental factors on genetic diversity of *Caragana microphylla* in Horqin sandy land, northeast China. *Ecology and Evolution* **6**: 8256–8266.

Hubisz,MJ, Falush D, Stephens M, Pritchard JK. 2009. Inferring weak population structure with the assistance of sample group information. *Molecular Ecology Resources* **9**: 1322–1332.

Hulton NRJ, Purves RS, McCulloch RD, Sugden DE, Bentley MJ. 2002. The Last Glacial Maximum and deglaciation in southern South America. *Quaternary Science Reviews* **21**: 233–241.

Jombart T. 2008. *adegenet*: a R package for the multivariate analysis of genetic markers. *Bioinformatics* **24**: 1403–1405.

Jombart T, Devillard S, Balloux F. 2010. Discriminant analysis of principal components: a new method for the analysis of genetically structured populations. *BMC Genetics* **11**: 94.

Jombart T, Devillard S, Dufour A-B, Pontier D. 2008. Revealing cryptic spatial patterns in genetic variability by a new multivariate method. *Heredity* **101**: 92–103.

Kadereit J. Westberg E. 2007. Determinants of phylogeographic structure: a comparative study of seven coastal flowering plant species across their European range. *Watsonia* **26**: 229–238.

Kamvar ZN, Brooks JC, Grünwald NJ. 2015. Novel R tools for analysis of genome-wide population genetic data with emphasis on clonality. *Frontiers in Genetics* **6**: 208.

Kamvar ZN, Tabima JF, Grünwald NJ. 2014. *Poppr*: an R package for genetic analysis of

599 populations with clonal, partially clonal, and/or sexual reproduction. *PeerJ* **2**: e281.

600 **Leal BSS, Palma da Silva C, Pinheiro F. 2016.** Phylogeographic studies depict the role of
601 space and time scales of plant speciation in a highly diverse Neotropical region. *Critical*
602 *Reviews in Plant Sciences* **35**: 215–230.

603 **Lee C-R, Mitchell-Olds T. 2011.** Quantifying effects of environmental and geographical
604 factors on patterns of genetic differentiation. *Molecular Ecology* **20**: 4631–4642.

605 **Loveless MD, Hamrick JL. 1984.** Ecological determinants of genetic structure in plant
606 populations. *Annual Review of Ecology and Systematics* **15**: 65–95.

607 **Mäder G, Fregonezi JN, Lorenz-Lemke AP, Bonatto SL, Freitas LB. 2013.** Geological
608 and climatic changes in Quaternary shaped the evolutionary history of *Calibrachoa*
609 *heterophylla*, an endemic South-Atlantic species of petunia. *BMC Evolutionary Biology*
610 **13**: 178.

611 **Mäder G, Freitas LB. 2019.** Biogeographical, ecological, and phylogenetic analyses
612 clarifying the evolutionary history of *Calibrachoa* in South American grasslands.
613 *Molecular Phylogenetics and Evolution* **141**: 106614.

614 **Manel S, Schwartz MK, Luikart G, Taberlet P. 2003.** Landscape genetics: combining
615 landscape ecology and population genetics. *Trends in Ecology & Evolution* **18**: 189–197.

616 **Martinho CT, Hesp PA, Dillenburg SR. 2010.** Morphological and temporal variations of
617 transgressive dune fields of the northern and mid-littoral Rio Grande do Sul coast,
618 Southern Brazil. *Geomorphology* **117**: 14–32.

619 **Massante JC, Gerhold P. 2020.** Environment and evolutionary history depict phylogenetic
620 alpha and beta diversity in the Atlantic coastal white-sand woodlands. *Journal of*
621 *Vegetation Science* **31**: 634-645.

622 **Meireles JE, Manos PS. 2018.** Pervasive migration across rainforest and sandy coastal plain
623 *Aechmea nudicaulis* (Bromeliaceae) populations despite contrasting environmental

624 conditions. *Molecular Ecology* **27**: 1261–1272.

625 **Meirmans PG. 2012.** The trouble with isolation by distance. *Molecular Ecology* **21**: 2839–
626 2846.

627 **Miller MA, Pfeiffer W, Schwartz T. 2010.** Creating the CIPRES Science Gateway for
628 inference of large phylogenetic trees. In: *2010 Gateway Computing Environments*
629 *Workshop (GCE)*. New Orleans: IEEE, 1–8.

630 **Miloslavich P, Klein E, Díaz JM, *et al.* 2011.** Marine biodiversity in the Atlantic and Pacific
631 coasts of South America: knowledge and gaps. *PLoS ONE* **6**: e14631.

632 **Möller OO, Castaing P. 1999.** Hydrographical characteristics of the estuarine area of Patos
633 Lagoon (30°S, Brazil). *In* Perillo GME, Piccolo MC, Pino-Quivira M, eds, *Estuaries of*
634 *South America*.Berlin: Springer, 83–100.

635 **Möller OO, Castaing P, Salomon JC, Lazure P. 2001.** The influence of local and non-local
636 forcing effects on the sub-tidal circulation of Patos Lagoon. *Estuaries* **24**: 297–311.

637 **Möller OO, Lorenzzentti JA, Stech JL,Math MM. 1996.** The Patos Lagoon summertime
638 circulation and dynamics. *Continental Shelf Research* **16**: 335–351.

639 **Mori GM, Zucchi MI, Sampaio I, Souza AP. 2015.** Species distribution and introgressive
640 hybridization of two *Avicennia* species from the Western Hemisphere unveiled by
641 phylogeographic patterns. *BMC Evolutionary Biology* **15**: 61.

642 **Nosil P, Funk PD, Ortiz-Barrientos D. 2009.** Divergent selection and heterogeneous
643 genomic divergence. *Molecular Ecology* **18**: 375–402.

644 **Nosil P, Vines TH, Funk DJ. 2005.** Reproductive isolation caused by natural selection
645 against immigrants from divergent habitats. *Evolution* **59**: 705–719.

646 **Oksanen J, Blanchet FG, Kindt R, *et al.* 2015.** *vegan*: community ecology package. R
647 package version 2.3-0. http://CRAN.R-project.org/package=vegan.

648 **Orsini L, Vanoverbeke J, Swillen I, Mergeay J, Meester L. 2013.** Drivers of population

genetic differentiation in the wild: isolation by dispersal limitation, isolation by adaptation and isolation by colonization. *Molecular Ecology* **22**: 5983–5999.

Pritchard JK, Stephens M, Donnelly P. 2000. Inference of population structure using multilocus genotype data. *Genetics* **155**: 945–959.

R Core Team. 2019. *R*: a language and environment for statistical computing. R Foundation for Statistical Computing, Vienna, Austria. http://www.R-project.org/.

Rambaut A, Suchard MA, Xie D, Drummond A. 2014. *Tracer* v1.6. http://beast.bio.ed.ac.uk/Tracer.

Ramos-Fregonezi AMC, Fregonezi JN, Cybis GB, Fagundes NJR, Bonatto SL, Freitas LB. 2015. Were sea level changes during the Pleistocene in the South Atlantic Coastal Plain a driver of speciation in *Petunia* (Solanaceae)? *BMC Evolutionary Biology* **15**: 92.

Rissler LJ. 2016. Union of phylogeography and landscape genetics. *Proceedings of the National Academy of Sciences USA* **113**: 8079–8086.

Rousset F. 1997. Genetic differentiation and estimation of gene flow from F-statistics under isolation by distance. *Genetics* **145**: 1219–1228.

Roy A, Frascaria N, MacKay J, Bousquet J. 1992. Segregating random amplified polymorphic DNAs (RAPDs) in *Betula alleghaniensis*. *Theoretical and Applied Genetics* **85**: 173–180.

Saillard M, Hall SR, Audin L, *et al.* 2009. Non-steady long-term uplift rates and Pleistocene marine terrace development along the Andean margin of Chile (31°S) inferred from 10Be dating. *Earth and Planetary Science Letters* **277**: 50–63.

Santos-Fischer CB, Corrêa ICS, Weschenfelder J, Torgan LC, Stone JR. 2016. Paleoenvironmental insights into the Quaternary evolution of the southern Brazilian coast based on fossil and modern diatom assemblages. *Palaeogeography, Palaeoclimatology, Palaeoecology* **446**: 108–124.

674 **Scarano FR. 2002.** Structure, function and floristic relationships of plant communities in
675 stressful habitats marginal to the Brazilian Atlantic Rainforest. *Annals of Botany* **90**: 517–
676 524.
677 **Schaal BA, Olsen KM. 2000.** Gene genealogies and population variation in plants.
678 *Proceedings of the National Academy of Sciences USA* **97**: 7024–7029.
679 **Schierenbeck KA. 2017.** Population-level genetic variation and climate change in a
680 biodiversity hotspot. *Annals of Botany* **119**: 215–228.
681 **Sérsic, AN, Cosacov A, Cocucci AA, *et al.* 2011.** Emerging phylogeographical patterns of
682 plants and terrestrial vertebrates from Patagonia. *Biological Journal of the Linnean*
683 *Society* **103**: 475–494.
684 **Sexton JP, Hangartner SB, Hoffmann AA. 2014.** Genetic isolation by environment or
685 distance: which pattern of gene flow is most common? *Evolution* **68**: 1–15.
686 **Silva GAR, Antonelli A, Lendel A, Moraes EM, Manfrin MH. 2018.** The impact of early
687 Quaternary climate change on the diversification and population dynamics of a South
688 American cactus species. *Journal of Biogeography* **45**: 76–88.
689 **Silva-Arias GA, Mäder G, Bonatto SL, Freitas LB. 2015.** Novel Microsatellites for
690 *Calibrachoa heterophylla* (Solanaceae) endemic to the South Atlantic Coastal Plain of
691 South America. *Applications in Plant Sciences* **3**: 1500021.
692 **Silva-Arias GA, Reck-Kortmann M, Carstens BC, Hasenack H, Bonatto SL, Freitas LB.**
693 **2017.** From inland to the coast: spatial and environmental signatures on the genetic
694 diversity in the colonization of the South Atlantic Coastal Plain. *Perspectives in Plant*
695 *Ecology, Evolution and Systematics* **28**: 47–57.
696 **Slatkin M. 1987.** Gene flow and the geographic structure of natural populations. *Science* **236**:
697 787–792.
698 **Sork VL. 2016.** Gene flow and natural selection shape spatial patterns of genes in tree

699 populations: implications for evolutionary processes and applications. *Evolutionary*
700 *Applications* **9**: 291–310.
701 **Spiegelhalter DJ, Best NG, Carlin BP, van der Linde A. 2002.** Bayesian measures of
702 model complexity and fit. *Journal of the Royal Statistical Society: Series B (Statistical*
703 *Methodology)* **64**: 583–639.
704 **Tellier F, Meynard AP, Correa JA, Faugeron S, Valero M. 2009.** Phylogeographic
705 analyses of the 30° S south-east Pacific biogeographic transition zone establish the
706 occurrence of a sharp genetic discontinuity in the kelp *Lessonia nigrescens*: vicariance or
707 parapatry? *Molecular Phylogenetics and Evolution* **53**: 679–693.
708 **Tellier F, Tapia J, Faugeron S, Destombe C, Valero M. 2011.** The *Lessonia nigrescens*
709 species complex (Laminariales, Phaeophyceae) shows strict parapatry and complete
710 reproductive isolation in a secondary contact zone: reproductive isolation between kelp
711 species. *Journal of Phycology* **47**: 894–903.
712 **Thompson JD. 1999.** Population differentiation in Mediterranean plants: insights into
713 colonization history and the evolution and conservation of endemic species. *Heredity* **82**:
714 229–236.
715 **Tomazelli LJ, Dillenburg SR. 2007.** Sedimentary facies and stratigraphy of a last
716 interglacial coastal barrier in south Brazil. *Marine Geology* **244**: 33–45.
717 **Tomazelli LJ, Dillenburg SR, Villwock JA. 2000.** Late Quaternary geological history of
718 Rio Grande do Sul coastal plain, southern Brazil. *Revista Brasileira de Geociências* **30**:
719 474–476.
720 **Turchetto-Zolet AC, Pinheiro F, Salgueiro F, Palma-Silva C. 2013.** Phylogeographical
721 patterns shed light on evolutionary process in South America. *Molecular Ecology* **22**:
722 1193–1213.
723 **van Oppen MJH, Rico C, Turner GF, Hewitt GM. 2000.** Extensive homoplasy, non-

724 stepwise mutations, and shared ancestral polymorphism at a complex microsatellite locus
725 in lake Malawi cichlids. *Molecular Biology and Evolution* **17**: 489–498.
726 **Wang IJ. 2013.** Examining the full effects of landscape heterogeneity on spatial genetic
727 variation: a multiple matrix regression approach for quantifying geographic and
728 ecological isolation. *Evolution* **67**: 3403–3411.
729 **Wang IJ, Bradburd GS. 2014.** Isolation by environment. *Molecular Ecology* **23**: 5649–
730 5662.
731 **Weir BS, Cockerham CC. 1984.** Estimating F-statistics for the analysis of population
732 structure. *Evolution* **38**: 1358–1370.
733 **Weschenfelder J, Baitelli R, Corrêa ICS, Bortolin EC, Santos CB. 2014.** Quaternary
734 incised valleys in southern Brazil coastal zone. *Journal of South American Earth Sciences*
735 **55**: 83–93.
736 **Weschenfelder J, Corrêa ICS, Aliotta S, Baitelli R. 2010.** Paleochannels related to Late
737 Quaternary sea-level changes in Southern Brazil. *Brazilian Journal of Oceanography* **58**:
738 35–44.
739 **Whigham PA, Dick GC, Spencer HG. 2008.** Genetic drift on networks: ploidy and the time
740 to fixation. *Theoretical Population Biology* **74**: 283–290.
741 **Wilson G, Rannala B. 2003.** Bayesian inference of recent migration rates using multilocus
742 genotypes. *Genetics* **163**: 1177-1191.

743

744 # TABLES

745 **Table 1.** Sampling information and inbreeding coefficients for *Calibrachoa heterophylla*

746 populations. Population ID codes follow Fig. 1A.

Pop ID	N	Location	Long	Lat	F_{IS}
1	4	São Francisco de Assis	-55.10077	-29.58307	-0.16
2	10	Cacequi 1	-54.85375	-29.8947	-0.01
3	9	Cacequi 2	-54.90852	-29.85478	0
4	27	Barra do Ribeiro	-51.20255	-30.40754	0.08
5	4	Arambaré	-51.49195	-30.90082	0.12
6	23	Pelotas	-52.16478	-31.70757	0.07
7	10	Laguna	-48.76501	-28.45991	0.34**
8	23	Torres	-49.79809	-29.43227	0.17**
9	37	S Antônio da Patrulha	-50.42936	-29.89291	0.10*
10	3	Mostardas 1	-50.73934	-30.93746	0.35
11	13	Mostardas 2	-50.90112	-31.10909	0.08
12	12	S José do Norte 1	-51.42576	-31.66673	-0.01
13	11	S José do Norte 2	-52.03612	-32.02393	-0.05
14	26	Rio Grande	-52.54661	-32.52396	0.27***
15	41	S Vitória do Palmar	-52.7323	-32.98765	0.25***

747

748 *P-value < 0.05; ** P-value < 0.01; *** P-value < 0.001

749

750 **Table 2.** Model support statistics (upper panel) and parameter estimations taken from the
751 best-supported model (lower panel).

Model name	Ln marginal Likelihood	Log Bayes Factor	Model probability
Step stone from coast	-5900.7	0	1.0
Source-sink from west	-5940.5	-79.6	5.1E-18
Source-sink from inland	-5941.5	-81.6	1.9E-18
Step stone from inland	-5944.9	-88.4	6.5E-20

Parameter	Median	Mean	95 % CI
Θ 'Inland'	4.11	4.25	2.55 - 6.28
Θ 'West'	0.55	0.56	0.12 - 0.96
Θ 'North'	0.51	0.52	0.05 - 0.95
Θ 'South'	0.27	0.22	0 - 0.55
M 'West' -> 'Inland'	0.41	0.45	0 - 1.16
M 'North' -> 'West'	0.3	0.26	0 - 0.6
M 'South' -> 'West'	0.19	0.08	0 - 0.41

752

753 Bayes factor values < 2 indicate a strong preference for the model with the highest probability. Θ = mutation
754 scaled population size; M = mutation scaled migration rate; CI = confidence interval. For graphical model
755 descriptions see Fig. S1.

756

757

758 **FIGURES**

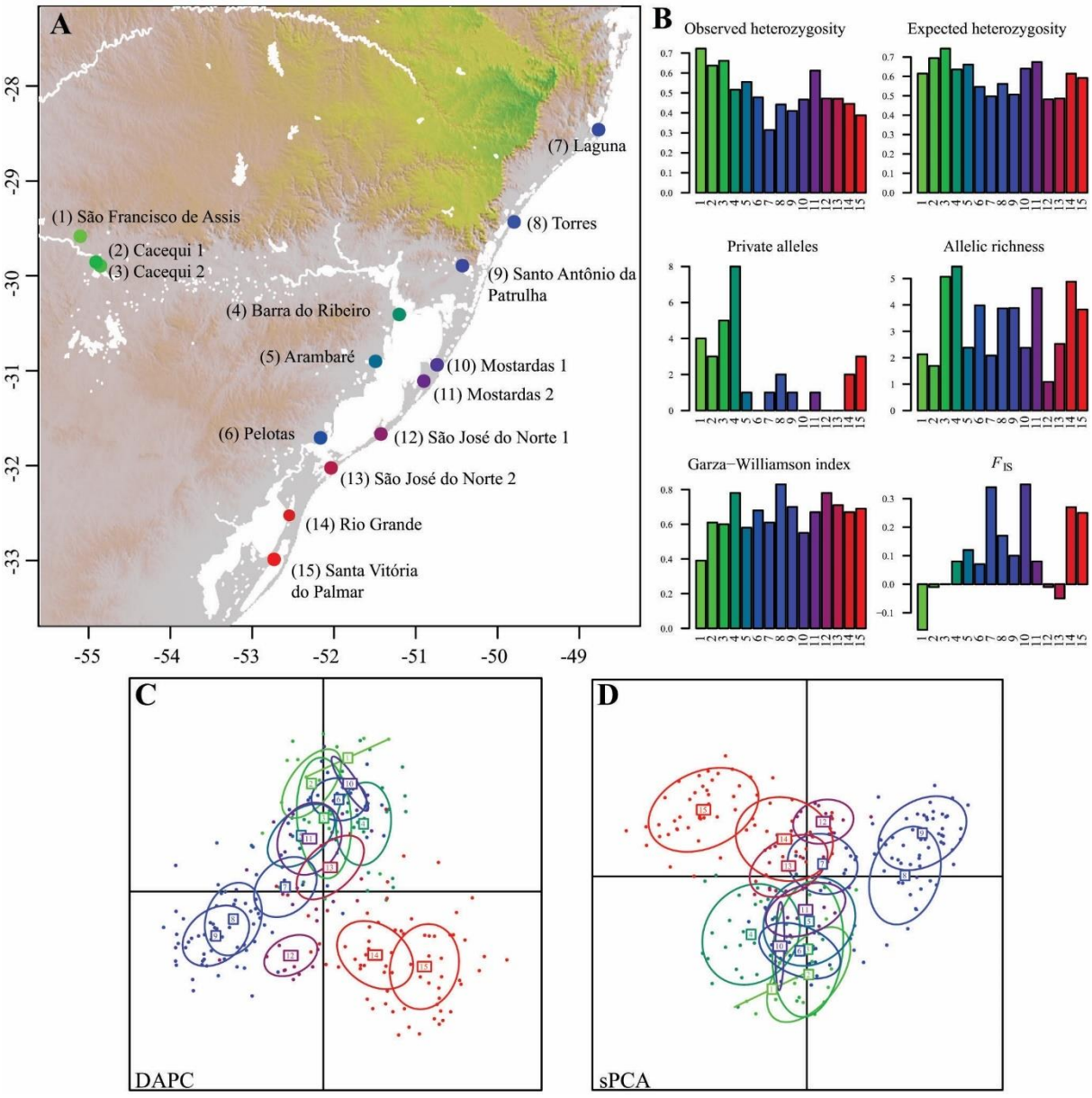

759

760 **Figure 1.** (A) Geographic locations of *Calibrachoa heterophylla* populations. (B) Graphical
761 representation of the mean genetic diversity statistics estimated for each population across all
762 microsatellite loci. (C) Scatterplot of the DAPC analysis. (D) Scatterplot of the sPCA.
763 Populations' numbers and colours follow each panel.

764

765

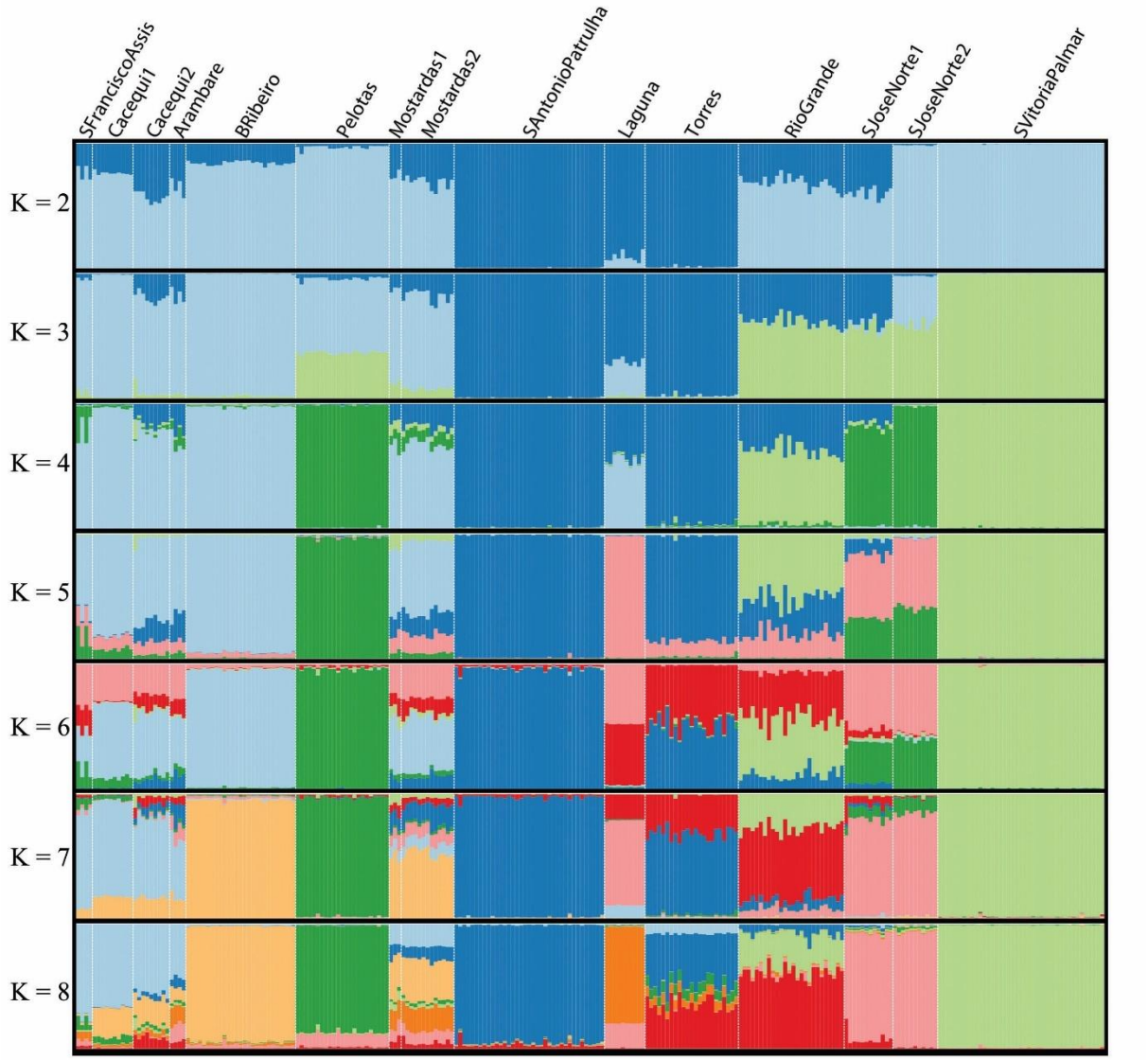

Figure 2. Bar plots of the individual membership for K = 2-8 genetic clusters as estimated with STRUCTURE. Populations are separated by white dashed lines and named on the figure top side of.

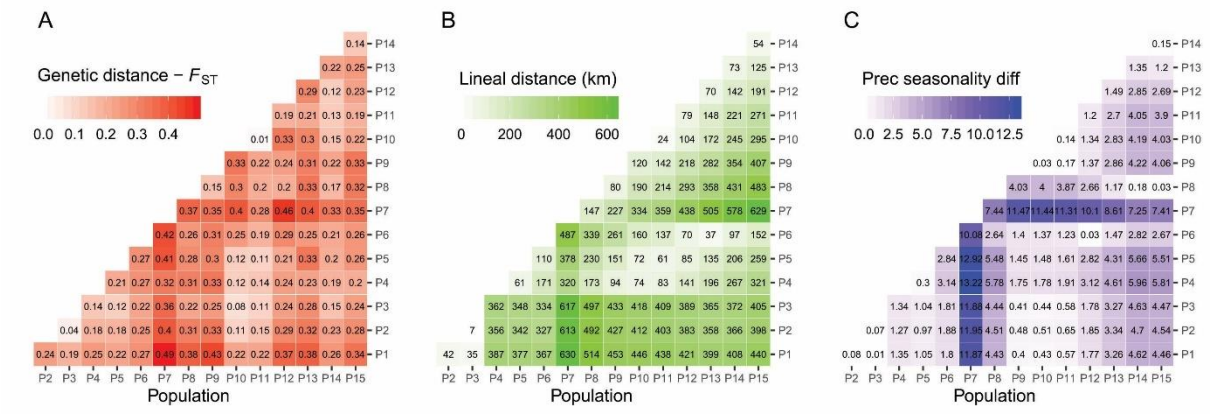

Figure 3. Interpopulation genetic, geographic, and environmental dissimilarity matrices. (A) Genetic differentiation and F_{ST}; (B) Linear geographic distance; (C) Precipitation seasonality dissimilarity. The values are represented by a colour on a continuous scale. Populations are numbered as in Fig. 1A and Table 1.

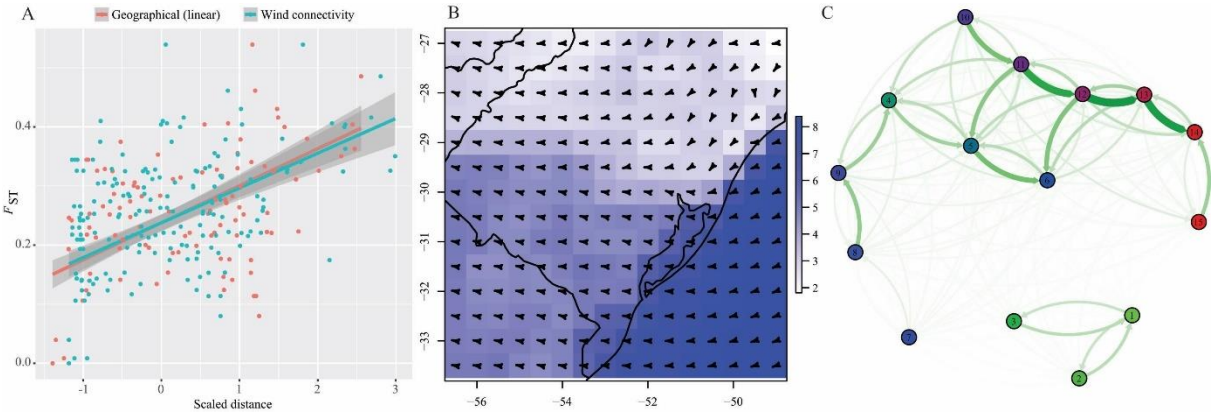

Figure 4. Spring season wind fields in the South Atlantic Coastal Plain and inference of wind in the population connectivity and gene flow. (A) Correlation between geographical distance (red) and wind connectivity (blue) coast distance matrices with the F_{ST} genetic distance matrix; (B) Mean values 2011-2016 of wind speed (blue scale m/s) and direction (arrows) for the spring season (Sept-Nov); (C) Inter-population wind connectivity network.

788 **SUPPLEMENTARY MATERIAL**

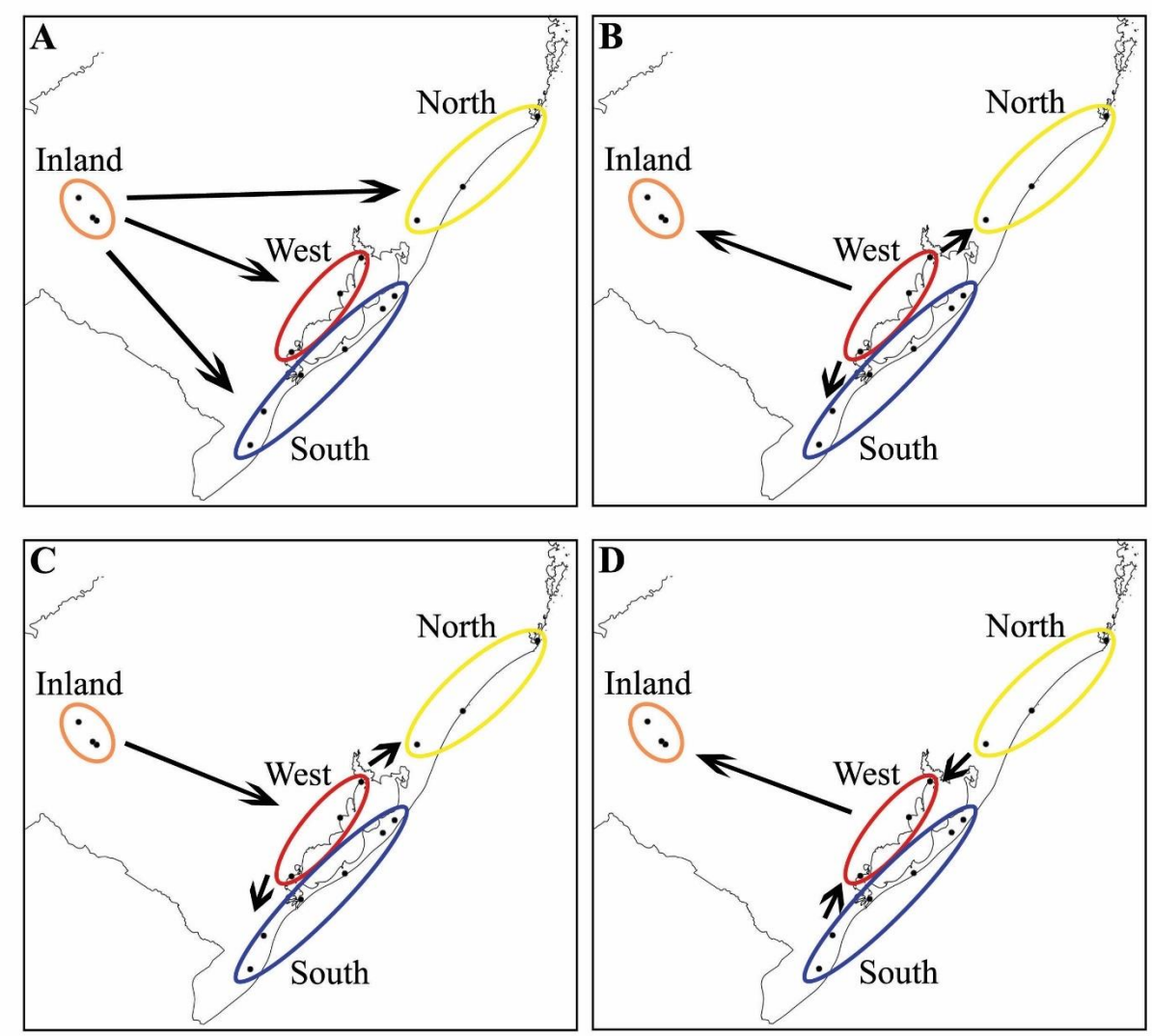

789

790 **Figure S1.** Graphical representation of the four coalescent migration models tested in

791 MIGRATE-N for *Calibrachoa heterophylla*. (A) Source-sink from inland; (B) Source-sink

792 from the west; (C) Step-stone from inland; (D) Step-stone from the coast.

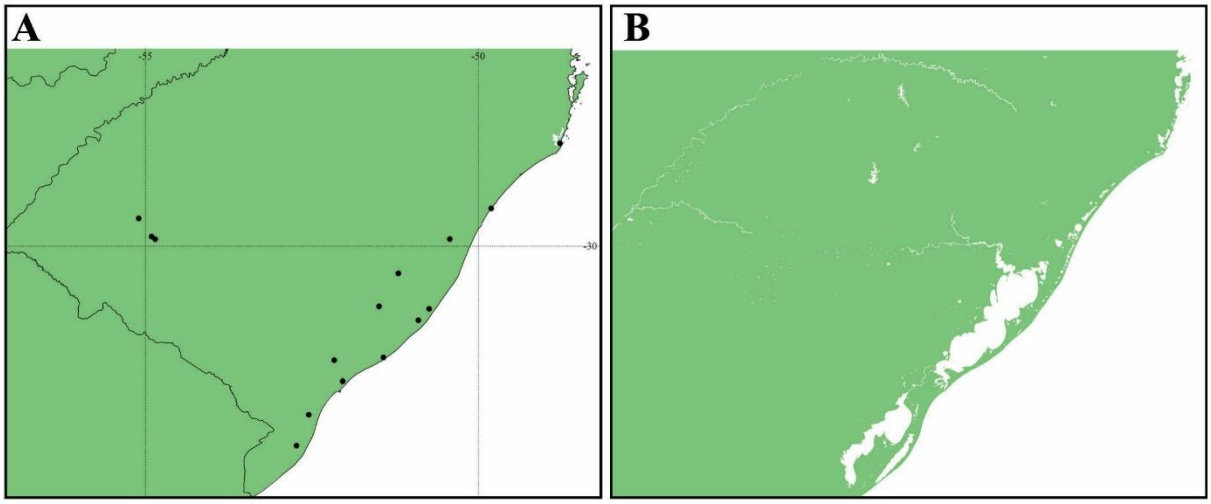

Figure S2. Graphical representation of the raster layers used to calculate the connectivity values in topographic tests (A) Continuous model; (B) Water bodies model.

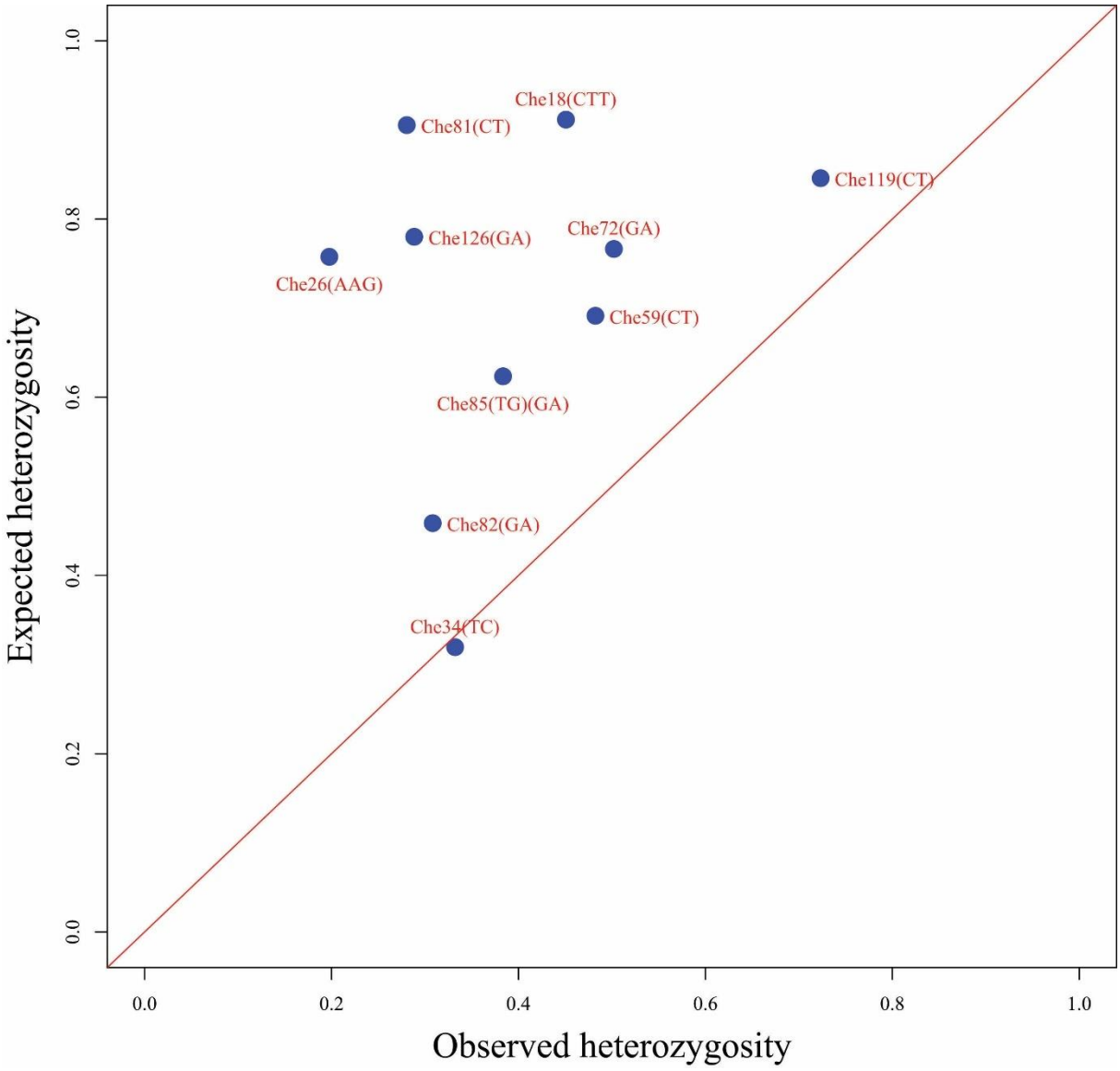

Figure S3. The plot of observed *vs*. expected heterozygosity for each locus.

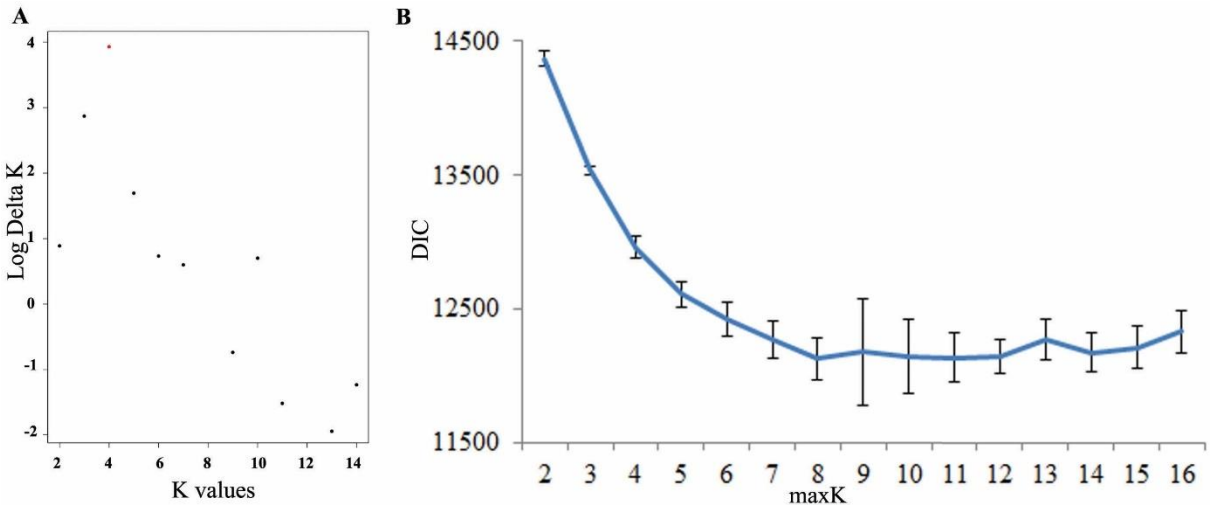

Figure S4. (A) Plots of the best K estimates for STRUCTURE results. (B) Plots of the mean and standard deviation of the deviance information criterion (DIC) obtained for each maxK assessed with TESS.

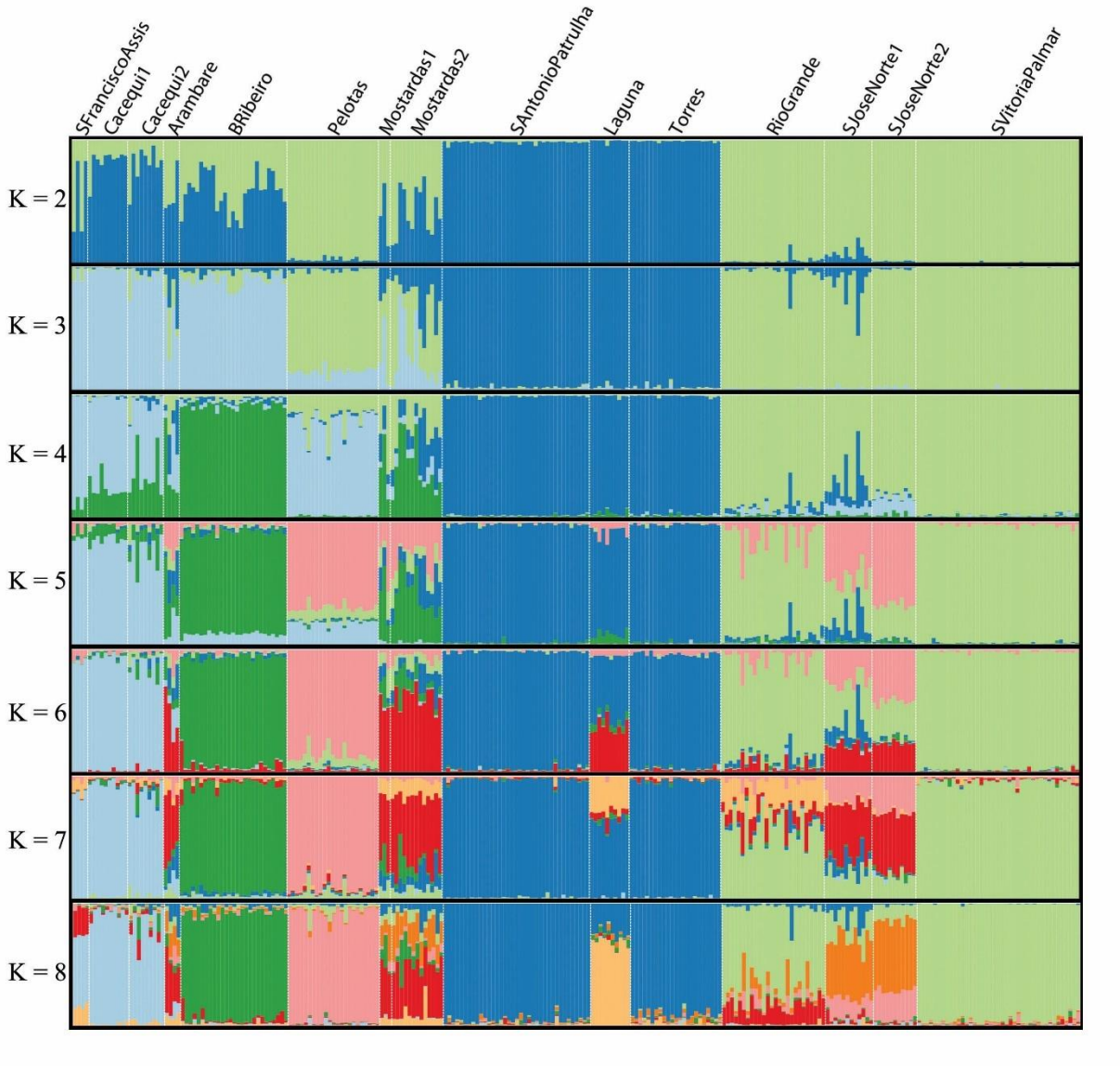

806

807 **Figure S5.** Bar plots of the individual membership for each genetic cluster obtained with

808 TESS. Populations are separated by white dashed lines and names are indicated on the figure

809 top side.

810

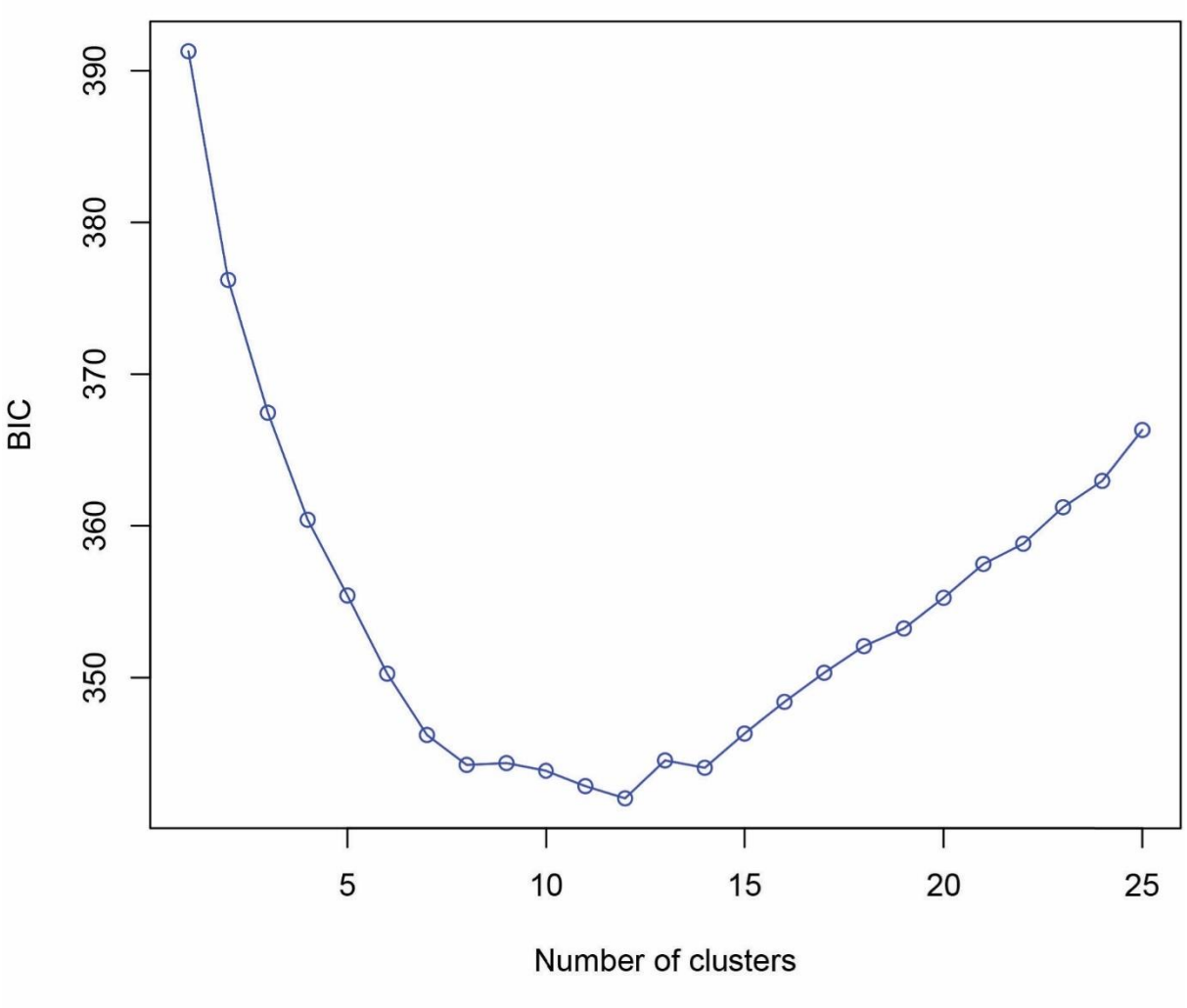

811

812 **Figure S6.** The plot of Bayesian information criterion (BIC) values obtained for each K

813 number as assessed with the multivariate method Discriminant Analyses of Principal

814 Components.

Table S1. Migration estimates obtained with three independent runs of BAYESASS. Populations are numbered as in Fig. 1. The values indicate the estimated posterior mean effective migration rate per generation [the fraction of individuals in population *i* (rows) that are migrants derived from population *j* (columns)] and the numbers in parenthesis show the standard deviation. Bold values indicate the diagonal (intra-population estimates) and red values indicate the highest migration estimates (those with above zero 95% confidence intervals).

	1_j	2_j	3_j	4_j	5_j	6_j	7_j	8_j	9_j	10_j	11_j	12_j	13_j	14_j	15_j
1_i	**0.6850 (0.0180)**	0.0454 (0.0389)	0.0179 (0.0171)	0.0183 (0.0185)	0.0177 (0.0168)	0.0330 (0.0280)	0.0179 (0.0169)	0.0405 (0.0306)	0.0175 (0.0164)	0.0179 (0.0168)	0.0186 (0.0183)	0.0181 (0.0172)	0.0176 (0.0169)	0.0173 (0.0164)	0.0174 (0.0164)
2_i	0.0136 (0.0132)	**0.7980 (0.0339)**	0.0136 (0.0129)	0.0134 (0.0131)	0.0136 (0.0131)	0.0168 (0.0153)	0.0136 (0.0130)	0.0160 (0.0155)	0.0135 (0.0130)	0.0173 (0.0159)	0.0168 (0.0159)	0.0135 (0.0130)	0.0135 (0.0131)	0.0135 (0.0130)	0.0133 (0.0126)
3_i	0.0144 (0.0139)	**0.1189 (0.0356)**	**0.6806 (0.0134)**	0.0140 (0.0134)	0.0211 (0.0185)	0.0140 (0.0133)	0.0140 (0.0133)	0.0232 (0.0199)	0.0144 (0.0137)	0.0139 (0.0131)	0.0146 (0.0142)	0.0153 (0.0145)	0.0138 (0.0132)	0.0140 (0.0132)	0.0138 (0.0132)
4_i	0.0175 (0.0169)	0.0203 (0.0192)	0.0174 (0.0164)	**0.6842 (0.0165)**	0.0179 (0.0171)	0.0189 (0.0178)	0.0174 (0.0165)	**0.0793 (0.0330)**	0.0177 (0.0167)	0.0175 (0.0167)	0.0177 (0.0169)	0.0174 (0.0168)	0.0179 (0.0170)	0.0212 (0.0195)	0.0176 (0.0167)
5_i	0.0080 (0.0079)	0.0101 (0.0094)	0.0079 (0.0077)	0.0081 (0.0080)	**0.8792 (0.0257)**	0.0080 (0.0079)	0.0080 (0.0079)	0.0105 (0.0100)	0.0080 (0.0079)	0.0087 (0.0085)	0.0086 (0.0083)	0.0081 (0.0078)	0.0081 (0.0078)	0.0105 (0.0099)	0.0082 (0.0081)
6_i	0.0088 (0.0087)	0.0088 (0.0086)	0.0088 (0.0087)	0.0087 (0.0085)	0.0089 (0.0087)	**0.8694 (0.0270)**	0.0089 (0.0086)	0.0098 (0.0095)	0.0087 (0.0085)	0.0088 (0.0086)	0.0087 (0.0087)	0.0092 (0.0089)	0.0088 (0.0085)	0.0149 (0.0124)	0.0088 (0.0085)
7_i	0.0185 (0.0175)	0.0181 (0.0175)	0.0187 (0.0176)	0.0186 (0.0173)	0.0191 (0.0177)	0.0193 (0.0181)	**0.6849 (0.0171)**	**0.0711 (0.0320)**	0.0187 (0.0177)	0.0187 (0.0179)	0.0185 (0.0178)	0.0203 (0.0194)	0.0185 (0.0175)	0.0186 (0.0178)	0.0183 (0.0175)
8_i	0.0119 (0.0114)	0.0119 (0.0113)	0.0122 (0.0117)	0.0120 (0.0116)	0.0138 (0.0134)	0.0123 (0.0117)	0.0121 (0.0117)	**0.8201 (0.0329)**	0.0119 (0.0115)	0.0129 (0.0126)	0.0138 (0.0131)	0.0143 (0.0134)	0.0119 (0.0116)	0.0156 (0.0144)	0.0134 (0.0131)
9_i	0.0063 (0.0063)	0.0065 (0.0064)	0.0064 (0.0064)	0.0064 (0.0063)	0.0064 (0.0064)	0.0065 (0.0063)	0.0065 (0.0065)	0.0066 (0.0064)	**0.9055 (0.0216)**	0.0064 (0.0061)	0.0086 (0.0086)	0.0086 (0.0078)	0.0064 (0.0063)	0.0064 (0.0063)	0.0065 (0.0064)
10_i	0.0132 (0.0127)	0.0134 (0.0131)	0.0133 (0.0127)	0.0136 (0.0134)	0.0134 (0.0127)	0.0135 (0.0126)	0.0133 (0.0129)	0.0136 (0.0131)	0.0135 (0.0127)	**0.7483 (0.0703)**	0.0768 (0.0705)	0.0136 (0.0130)	0.0133 (0.0129)	0.0135 (0.0129)	0.0138 (0.0133)
11_i	0.0088 (0.0085)	0.0087 (0.0084)	0.0088 (0.0086)	0.0088 (0.0086)	0.0088 (0.0085)	0.0088 (0.0086)	0.0088 (0.0084)	0.0088 (0.0085)	0.0973 (0.0967)	0.0094 (0.0090)	**0.7873 (0.0966)**	0.0095 (0.0092)	0.0088 (0.0086)	0.0087 (0.0085)	0.0086 (0.0086)
12_i	0.0081 (0.0080)	0.0081 (0.0080)	0.0081 (0.0079)	0.0081 (0.0080)	0.0081 (0.0079)	0.0087 (0.0083)	0.0080 (0.0079)	0.0088 (0.0085)	0.0098 (0.0094)	0.0082 (0.0078)	0.0088 (0.0086)	**0.8814 (0.0253)**	0.0081 (0.0080)	0.0085 (0.0083)	0.0092 (0.0089)
13_i	0.0122 (0.0117)	0.0124 (0.0120)	0.0125 (0.0120)	0.0125 (0.0123)	0.0124 (0.0119)	0.0124 (0.0120)	0.0122 (0.0118)	0.0131 (0.0126)	0.0136 (0.0133)	0.0125 (0.0119)	0.0125 (0.0120)	0.0143 (0.0136)	**0.6792 (0.0121)**	**0.1557 (0.0323)**	0.0125 (0.0120)
14_i	0.0127 (0.0121)	0.0125 (0.0122)	0.0129 (0.0124)	0.0129 (0.0125)	0.0127 (0.0121)	0.0150 (0.0144)	0.0130 (0.0123)	0.0131 (0.0126)	0.0129 (0.0123)	0.0127 (0.0124)	0.0129 (0.0124)	0.0129 (0.0124)	0.0127 (0.0122)	**0.8180 (0.0322)**	0.0130 (0.0126)
15_i	0.0060 (0.0059)	0.0059 (0.0058)	0.0059 (0.0058)	0.0060 (0.0058)	0.0059 (0.0059)	0.0061 (0.0060)	0.0060 (0.0058)	0.0060 (0.0060)	0.0059 (0.0058)	0.0059 (0.0058)	0.0059 (0.0058)	0.0061 (0.0060)	0.0060 (0.0059)	0.0059 (0.0058)	**0.9164 (0.0193)**

	1_j	2_j	3_j	4_j	5_j	6_j	7_j	8_j	9_j	10_j	11_j	12_j	13_j	14_j	15_j
1_i	**0.6848 (0.0172)**	0.0418 (0.0393)	0.0399 (0.0400)	0.0175 (0.0163)	0.0175 (0.0165)	0.0262 (0.0246)	0.0178 (0.0169)	0.0306 (0.0289)	0.0176 (0.0164)	0.0192 (0.0188)	0.0174 (0.0166)	0.0176 (0.0167)	0.0174 (0.0164)	0.0174 (0.0165)	0.0173 (0.0166)
2_i	0.0135 (0.0132)	**0.7976 (0.0340)**	0.0145 (0.0139)	0.0138 (0.0135)	0.0138 (0.0131)	0.0166 (0.0153)	0.0132 (0.0126)	0.0154 (0.0146)	0.0132 (0.0126)	0.0203 (0.0179)	0.0142 (0.0134)	0.0134 (0.0129)	0.0135 (0.0131)	0.0134 (0.0127)	0.0136 (0.0129)
3_i	0.0138 (0.0132)	**0.1111 (0.0383)**	**0.6858 (0.0186)**	0.0139 (0.0133)	0.0235 (0.0197)	0.0138 (0.0131)	0.0140 (0.0138)	0.0236 (0.0202)	0.0143 (0.0137)	0.0143 (0.0137)	0.0148 (0.0140)	0.0151 (0.0144)	0.0141 (0.0136)	0.0140 (0.0134)	0.0140 (0.0134)
4_i	0.0175 (0.0167)	0.0204 (0.0189)	0.0179 (0.0172)	**0.6839 (0.0163)**	0.0173 (0.0167)	0.0192 (0.0180)	0.0176 (0.0168)	**0.0805 (0.0335)**	0.0175 (0.0170)	0.0170 (0.0163)	0.0182 (0.0175)	0.0175 (0.0166)	0.0177 (0.0169)	0.0201 (0.0185)	0.0176 (0.0167)
5_i	0.0080 (0.0077)	0.0097 (0.0093)	0.0091 (0.0087)	0.0080 (0.0079)	**0.8789 (0.0260)**	0.0082 (0.0081)	0.0080 (0.0079)	0.0101 (0.0097)	0.0081 (0.0080)	0.0093 (0.0091)	0.0082 (0.0080)	0.0081 (0.0079)	0.0080 (0.0078)	0.0104 (0.0096)	0.0079 (0.0078)
6_i	0.0087 (0.0086)	0.0089 (0.0086)	0.0087 (0.0085)	0.0087 (0.0084)	0.0089 (0.0086)	**0.8697 (0.0270)**	0.0088 (0.0085)	0.0099 (0.0096)	0.0088 (0.0085)	0.0086 (0.0085)	0.0088 (0.0085)	0.0091 (0.0088)	0.0087 (0.0085)	0.0149 (0.0124)	0.0088 (0.0085)
7_i	0.0186 (0.0174)	0.0186 (0.0175)	0.0187 (0.0176)	0.0181 (0.0174)	0.0186 (0.0176)	0.0189 (0.0181)	**0.6854 (0.0178)**	**0.0713 (0.0319)**	0.0182 (0.0171)	0.0188 (0.0176)	0.0184 (0.0175)	0.0202 (0.0190)	0.0185 (0.0177)	0.0188 (0.0180)	0.0188 (0.0178)
8_i	0.0118 (0.0114)	0.0120 (0.0118)	0.0119 (0.0116)	0.0118 (0.0113)	0.0138 (0.0132)	0.0124 (0.0119)	0.0116 (0.0114)	**0.8204 (0.0323)**	0.0121 (0.0115)	0.0135 (0.0128)	0.0137 (0.0131)	0.0143 (0.0137)	0.0119 (0.0115)	0.0154 (0.0144)	0.0134 (0.0128)
9_i	0.0065 (0.0064)	0.0064 (0.0062)	0.0065 (0.0065)	0.0064 (0.0063)	0.0066 (0.0063)	0.0064 (0.0063)	0.0064 (0.0063)	0.0066 (0.0064)	**0.9034 (0.0216)**	0.0064 (0.0064)	0.0102 (0.0097)	0.0090 (0.0080)	0.0065 (0.0064)	0.0064 (0.0063)	0.0064 (0.0062)
10_i	0.0134 (0.0128)	0.0133 (0.0126)	0.0132 (0.0126)	0.0132 (0.0127)	0.0133 (0.0127)	0.0135 (0.0132)	0.0135 (0.0130)	0.0138 (0.0130)	0.0132 (0.0127)	**0.8033 (0.0452)**	0.0219 (0.0358)	0.0135 (0.0130)	0.0135 (0.0129)	0.0133 (0.0129)	0.0140 (0.0133)
11_i	0.0087 (0.0085)	0.0090 (0.0087)	0.0088 (0.0086)	0.0088 (0.0087)	0.0088 (0.0084)	0.0089 (0.0087)	0.0086 (0.0084)	0.0088 (0.0086)	0.0244 (0.0399)	0.0097 (0.0093)	**0.8593 (0.0457)**	0.0096 (0.0093)	0.0088 (0.0085)	0.0088 (0.0087)	0.0090 (0.0087)
12_i	0.0082 (0.0079)	0.0081 (0.0079)	0.0082 (0.0080)	0.0083 (0.0080)	0.0081 (0.0079)	0.0088 (0.0084)	0.0082 (0.0079)	0.0089 (0.0086)	0.0097 (0.0092)	0.0082 (0.0081)	0.0096 (0.0092)	**0.8802 (0.0255)**	0.0081 (0.0079)	0.0086 (0.0083)	0.0090 (0.0086)
13_i	0.0123 (0.0119)	0.0123 (0.0119)	0.0122 (0.0118)	0.0123 (0.0117)	0.0123 (0.0119)	0.0122 (0.0116)	0.0123 (0.0116)	0.0133 (0.0126)	0.0135 (0.0131)	0.0123 (0.0118)	0.0129 (0.0125)	0.0144 (0.0137)	**0.6790 (0.0117)**	**0.1564 (0.0318)**	0.0124 (0.0120)
14_i	0.0130 (0.0125)	0.0128 (0.0125)	0.0128 (0.0121)	0.0128 (0.0124)	0.0130 (0.0125)	0.0149 (0.0141)	0.0126 (0.0122)	0.0129 (0.0123)	0.0128 (0.0122)	0.0129 (0.0125)	0.0132 (0.0128)	0.0128 (0.0124)	0.0126 (0.0120)	**0.8182 (0.0322)**	0.0128 (0.0123)
15_i	0.0059 (0.0059)	0.0060 (0.0058)	0.0060 (0.0059)	0.0059 (0.0058)	0.0059 (0.0058)	0.0061 (0.0060)	0.0060 (0.0060)	0.0061 (0.0060)	0.0061 (0.0060)	0.0060 (0.0058)	0.0060 (0.0058)	0.0062 (0.0062)	0.0060 (0.0057)	0.0061 (0.0061)	**0.9157 (0.0194)**

	1_j	2_j	3_j	4_j	5_j	6_j	7_j	8_j	9_j	10_j	11_j	12_j	13_j	14_j	15_j
1_i	**0.6852 (0.0185)**	0.0557 (0.0411)	0.0219 (0.0246)	0.0177 (0.0170)	0.0175 (0.0167)	0.0259 (0.0244)	0.0178 (0.0169)	0.0338 (0.0299)	0.0174 (0.0164)	0.0187 (0.0180)	0.0180 (0.0177)	0.0175 (0.0167)	0.0177 (0.0167)	0.0178 (0.0171)	0.0175 (0.0164)
2_i	0.0134 (0.0130)	**0.7989 (0.0338)**	0.0139 (0.0132)	0.0135 (0.0128)	0.0136 (0.0131)	0.0171 (0.0158)	0.0134 (0.0129)	0.0156 (0.0150)	0.0133 (0.0130)	0.0179 (0.0165)	0.0156 (0.0149)	0.0133 (0.0127)	0.0135 (0.0128)	0.0135 (0.0130)	0.0135 (0.0131)
3_i	0.0143 (0.0136)	**0.1194 (0.0364)**	**0.6813 (0.0143)**	0.0139 (0.0133)	0.0211 (0.0188)	0.0139 (0.0132)	0.0137 (0.0133)	0.0222 (0.0196)	0.0143 (0.0138)	0.0142 (0.0137)	0.0146 (0.0141)	0.0150 (0.0144)	0.0139 (0.0133)	0.0141 (0.0135)	0.0140 (0.0135)
4_i	0.0176 (0.0167)	0.0207 (0.0194)	0.0174 (0.0165)	**0.6845 (0.0168)**	0.0176 (0.0170)	0.0185 (0.0175)	0.0175 (0.0168)	**0.0801 (0.0331)**	0.0177 (0.0167)	0.0176 (0.0168)	0.0177 (0.0169)	0.0175 (0.0165)	0.0174 (0.0162)	0.0209 (0.0192)	0.0172 (0.0164)
5_i	0.0081 (0.0079)	0.0099 (0.0093)	0.0081 (0.0079)	0.0082 (0.0078)	**0.8791 (0.0253)**	0.0081 (0.0079)	0.0080 (0.0079)	0.0104 (0.0099)	0.0080 (0.0079)	0.0088 (0.0085)	0.0083 (0.0081)	0.0083 (0.0081)	0.0080 (0.0078)	0.0104 (0.0097)	0.0082 (0.0079)
6_i	0.0088 (0.0086)	0.0088 (0.0085)	0.0087 (0.0086)	0.0088 (0.0087)	0.0087 (0.0086)	**0.8698 (0.0270)**	0.0089 (0.0084)	0.0097 (0.0092)	0.0088 (0.0086)	0.0087 (0.0084)	0.0088 (0.0086)	0.0091 (0.0086)	0.0087 (0.0083)	0.0148 (0.0122)	0.0088 (0.0086)
7_i	0.0185 (0.0178)	0.0186 (0.0178)	0.0183 (0.0172)	0.0184 (0.0175)	0.0188 (0.0178)	0.0194 (0.0185)	**0.6848 (0.0173)**	**0.0720 (0.0326)**	0.0183 (0.0172)	0.0183 (0.0172)	0.0188 (0.0179)	0.0202 (0.0187)	0.0185 (0.0177)	0.0187 (0.0177)	0.0183 (0.0175)
8_i	0.0120 (0.0115)	0.0120 (0.0115)	0.0117 (0.0114)	0.0119 (0.0117)	0.0138 (0.0134)	0.0123 (0.0118)	0.0119 (0.0116)	**0.8204 (0.0323)**	0.0121 (0.0117)	0.0132 (0.0128)	0.0139 (0.0133)	0.0141 (0.0132)	0.0119 (0.0116)	0.0154 (0.0145)	0.0133 (0.0128)
9_i	0.0065 (0.0065)	0.0064 (0.0063)	0.0064 (0.0063)	0.0065 (0.0064)	0.0065 (0.0064)	0.0064 (0.0062)	0.0065 (0.0063)	0.0065 (0.0065)	**0.9046 (0.0216)**	0.0065 (0.0063)	0.0091 (0.0089)	0.0086 (0.0079)	0.0064 (0.0063)	0.0065 (0.0063)	0.0066 (0.0064)
10_i	0.0132 (0.0126)	0.0133 (0.0127)	0.0133 (0.0127)	0.0132 (0.0127)	0.0136 (0.0129)	0.0134 (0.0129)	0.0134 (0.0126)	0.0135 (0.0132)	0.0133 (0.0127)	**0.7636 (0.0693)**	0.0623 (0.0674)	0.0136 (0.0130)	0.0132 (0.0126)	0.0133 (0.0130)	0.0139 (0.0133)
11_i	0.0087 (0.0085)	0.0088 (0.0086)	0.0088 (0.0087)	0.0087 (0.0085)	0.0086 (0.0084)	0.0090 (0.0087)	0.0087 (0.0084)	0.0089 (0.0087)	0.0836 (0.0938)	0.0092 (0.0089)	**0.8010 (0.0933)**	0.0092 (0.0089)	0.0087 (0.0084)	0.0089 (0.0090)	0.0090 (0.0087)
12_i	0.0081 (0.0078)	0.0083 (0.0081)	0.0081 (0.0079)	0.0083 (0.0080)	0.0082 (0.0079)	0.0088 (0.0086)	0.0083 (0.0081)	0.0088 (0.0085)	0.0098 (0.0095)	0.0080 (0.0080)	0.0090 (0.0089)	**0.8810 (0.0253)**	0.0081 (0.0079)	0.0084 (0.0083)	0.0089 (0.0086)
13_i	0.0123 (0.0116)	0.0125 (0.0120)	0.0123 (0.0118)	0.0125 (0.0120)	0.0124 (0.0118)	0.0124 (0.0117)	0.0121 (0.0117)	0.0128 (0.0123)	0.0132 (0.0125)	0.0125 (0.0121)	0.0129 (0.0125)	0.0145 (0.0136)	**0.6792 (0.0121)**	**0.1560 (0.0322)**	0.0124 (0.0122)
14_i	0.0129 (0.0126)	0.0127 (0.0123)	0.0128 (0.0123)	0.0129 (0.0124)	0.0129 (0.0124)	0.0150 (0.0142)	0.0129 (0.0124)	0.0130 (0.0127)	0.0129 (0.0123)	0.0127 (0.0122)	0.0130 (0.0124)	0.0130 (0.0126)	0.0128 (0.0121)	**0.8176 (0.0324)**	0.0129 (0.0124)
15_i	0.0059 (0.0058)	0.0060 (0.0059)	0.0059 (0.0058)	0.0061 (0.0060)	0.0059 (0.0060)	0.0060 (0.0058)	0.0060 (0.0059)	0.0060 (0.0060)	0.0059 (0.0058)	0.0058 (0.0058)	0.0061 (0.0059)	0.0060 (0.0059)	0.0059 (0.0059)	0.0059 (0.0057)	**0.9165 (0.0192)**